END
FILMED

MICROCOPY RESOLUTION TEST CHART
NATIONAL BUREAU OF STANDARDS-1963-A

RADC-TR-82-337
In-House Report
January 1983
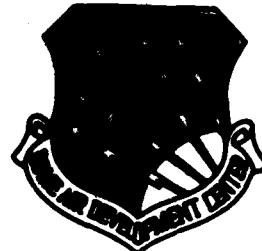
TWO-LAYER MODEL OF LINE-OF-SIGHT REFRACTIVE MULTIPATH PROPAGATION

Koichi Mano

DTIC
SELECTED
JUL 2 0 1983

A

ROME AIR DEVELOPMENT CENTER
Air Force Systems Command
Griffiss Air Force Base, NY 13441

DTIC FILE COPY

This report has been reviewed by the RADC Public Affairs Office (PA) and is releasable to the National Technical Information Service (NTIS). At NTIS it will be releasable to the general public, including foreign nations.

RADC-TR-82-337 has been reviewed and is approved for publication.

APPROVED:

TERENCE J. ELKINS
Chief, Propagation Branch
Electromagnetic Sciences Division

APPROVED:

ALLAN C. SCHELL
Chief, Electromagnetic Sciences Division

FOR THE COMMANDER:

JOHN ᴸ. HUSS
Acting Chief, Plans Office

SECURITY CLASSIFICATION OF THIS PAGE (When Data Entered)

REPORT DOCUMENTATION PAGE		READ INSTRUCTIONS BEFORE COMPLETING FORM
1. REPORT NUMBER RADC-TR-82-337	2. GOVT ACCESSION NO. AD.A130474	3. RECIPIENT'S CATALOG NUMBER 82-548
4. TITLE (and Subtitle) TWO-LAYER MODEL OF LINE-OF-SIGHT REFRACTIVE MULTIPATH PROPAGATION		5. TYPE OF REPORT & PERIOD COVERED In-House
		6. PERFORMING ORG. REPORT NUMBER
7. AUTHOR(s) Koichi Mano		8. CONTRACT OR GRANT NUMBER(s)
9. PERFORMING ORGANIZATION NAME AND ADDRESS Rome Air Development Center (EEP) Hanscom AFB Massachusetts 01731		10. PROGRAM ELEMENT PROJECT TASK AREA & WORK UNIT NUMBERS 62702F 46001607
11. CONTROLLING OFFICE NAME AND ADDRESS Rome Air Development Center (EEP) Hanscom AFB Massachusetts 01731		12. REPORT DATE January 1983
		13. NUMBER OF PAGES 56
14. MONITORING AGENCY NAME & ADDRESS(if different from Controlling Office)		15. SECURITY CLASS. (of this report) Unclassified
		15a. DECLASSIFICATION DOWNGRADING SCHEDULE

16. DISTRIBUTION STATEMENT (of this Report)

Approved for public release; distribution unlimited.

17. DISTRIBUTION STATEMENT (of the abstract entered in Block 20, if different from Report)

18. SUPPLEMENTARY NOTES

19. KEY WORDS (Continue on reverse side if necessary and identify by block number)

Line-of-sight refractive multipath
Two-layer model of multipath
Earth-flattening and ray-straightening systems
Angles of take-off and arrival
Amplitude factor

20. ABSTRACT (Continue on reverse side if necessary and identify by block number)

The two-layer model of the line-of-sight refractive multipath propagation was examined by employing the earth-flattening system of coordinates and the result was compared with an unpublished result carried out by other workers who studied the problem in the ray-straightening system. That these results should be identical is self-evident in principle provided the analysis is carried out rigorously. However, different approximations are used in the two methods, so it must still be demonstrated that the two methods given the same

(over)

DD FORM 1473 EDITION OF 1 NOV 65 IS OBSOLETE

20. Abstract (Contd)

result in practice as well as in theory. This report shows this equivalence in practice.

The atmosphere is assumed to consist of two layers. The lower layer, which is immediately above the earth's surface, is a non-ducting one, typically the standard atmosphere, with a constant thickness, and the upper one is a ducting layer of sufficient thickness. On the condition that the height above the earth's surface and the elevation angle of the ray remain sufficiently small throughout the ray trajectory, it can be shown that the ray path in either layer may be approximated as a circular arc of appropriate radius. Using this condition, one can derive a set of equations that can be used to determine the shape of the ray paths. The equation for the angle of take-off or arrival that follows from the set and comes in the form of a quartic equation can sometimes have more than one acceptable solution. The collection of these solutions that have, in general, different angles and times of arrival with different relative intensities can be considered to represent the multipath for the link under consideration.

A comparison of our quartic equation from the Earth Flattening Method with the similar equation obtained from the Ray-Straightening Method shows that the two equations are essentially identical. Moreover, the results for the transit time between the terminals and the intensity of the received signals are also shown to be essentially the same. Thus, the predictions for the multipath phenomenon by the earth-flattening and the ray-straightening methods were shown to produce the equivalent results that they should produce.

Contents

Illustrations

Table

Two-Layer Model of Line-of-Sight
Refractive Multipath Propagation

1. INTRODUCTION

The theoretical investigation of line-of-sight (LOS) refractive multipath propagation has not attracted much attention in the past in spite of the experimental evidences that support its existence. Perhaps the first noteworthy effort on this subject can be found in the work of Ruthroff.[1] He assumed that the earth's atmosphere consists of several concentric layers, each of which has a constant but different gradient of the index of refraction. In particular, he examined a two-layer atmosphere in some detail. This model has the obvious advantages of physical and mathematical simplicity. Here, the lower layer, which is immediately above the earth's surface, consists of the standard atmosphere, while the upper layer is a ducting layer of sufficiently large thickness. This model, although overly simplified, seems to deserve a more detailed study because it helps give us insight into the physics of LOS multipath propagation. Most of this report will be devoted to drawing inferences from this model in a systematic fashion.

1. Ruthroff, C. L. (1971) Multiple-path fading on line-of-sight microwave radio systems as a function of path length and frequency, Bell System Technical Journal 50(No. 7):2375-2398.

Several years after the appearance of Ruthroff's work, Pickering and DeRosa[2] placed his ideas in a more precise mathematical framework. Instead of working in the actual earth coordinate system, these authors chose to transform the actual geometry into the frame of reference in which the earth's surface is flat. This procedure will be referred to as the earth-flattening method (EFM). However, the work of Pickering and DeRosa[2] is incomplete because it does not cover all the conceivable relative orientations of the transmitter and receiver. Moreover, the two orientations they considered explicitly had to be treated individually because no unified set of equations could be found that can cover both of them.

A. Málaga and S. Parl[3] of Signatron, Inc. treated the problem by transforming the actual situation to the frame of reference in which the ray trajectory is piecewise straight. This procedure will be called the Ray-Straightening Method (RSM).

Since the EFM and RSM represent two avenues through which one and the same phenomenon can be examined it is clear in principle that they produce exactly the same result provided that they are followed through rigorously. In practice, however, approximations are made in both methods, so the two methods cannot be expected to lead to exactly same results, although they should be almost equivalent.

In this report, we will adopt the EFM, remedy the incompleteness in Ref. 2 mentioned earlier, and then show the equivalence of our results to those of Ref. 3 where the RSM has been employed. We believe that establishing such an equivalence once and for all in concrete terms will be a worthwhile endeavor. It should be noted that one can observe certain connections between the EFM and RSM predictions even before doing any detailed examination. Specifically, we refer to the relation that geometrically the roles of the ray trajectory and the layer boundary are interchanged in the two methods. This arises from the fact that in the real geometry the ray trajectory segment within each of the two layers may be approximated by an appropriate circular arc because the elevation angle of the ray path remains sufficiently small throughout the entirety of the ray trajectory. The mirror image relationship mentioned above leads to the prediction that the angles

2. Pickering, L.W., and DeRosa, J.K. (1979) Refractive multipath model for line-of-sight microwave relay links, IEEE Trans. on Comm. Com-27(No. 3): 1174-1182.

3. Málaga, A., and Parl, S. (1981) Theoretical Analysis of Microwave Propagation, Interim Scientific Report, Contract F19628-80-C-0106, Signatron, Inc. (The findings on multipath propagation contained in this report are included in a paper by S. Parl, "Characterization of multipath parameters for tropospheric microwave application" submitted to IEEE Trans. Antennas Propag.)

of take-off and arrival in the two methods should be equal, although the essential equality of the delay times may not be deduced in such a self-evident manner.

2. LINE-OF-SIGHT REFRACTIVE MULTIPATH PROPAGATION

We assume a two-layer system in which the lower layer is the standard atmosphere while the upper one is a ducting layer with a refractive-index gradient less than $-1/a \approx -157$ N unit/km, where a is the earth' radius. For a transmitter (T_x) and a receiver (R_x) in either one of the two layers, we will be concerned with the study by the EFM of the propagation of signals between them. As was mentioned in the Introduction, the work in Ref. 2 is incomplete in the sense that it does not cover all the possible orientations of the terminals relative to the interface between the two layers. After including all possible relative locations, we will obtain a unified set of equations to determine the geometry (and hence the angles of take-off and arrival) of a ray trajectory, and will indicate that the associated trajectory angles as determined by the EFM and RSM are essentially identical.

Then, the time of arrival calculated by the EFM will be compared with that due to the RSM to show that they are equivalent.

Finally, the amplitude factors of the received signal calculated by the two methods will be shown to be essentially equivalent also.

2.1 Angles of Take-Off and Arrival

In Ref. 2, the authors assumed that the height of R_x is not smaller than that of T_x, and considered two cases. In the first, T_x is in the lower layer and R_x is in the upper layer (Condition "A") and in the second, both terminals are found in the lower layer (Condition "B"). Obviously, this is not a complete description of the problem. Another terminal configuration in which both are in the upper layer (Condition "C"), must be added to the system. Completeness is also contingent on the understanding that the case in which T_x has greater height than R_x can be handled by applying the reciprocity theorem. In this report, Conditions "A", "B", and so forth in Ref. 2, will be designated as case (A), case (B), and so forth.

2.1.1 UNIFIED SET OF EQUATIONS FOR THE NONDIRECT PATHS

Consider a transmitter at T_x and a receiver at R_x separated by a distance L along the earth's surface. Let the heights of T_x, R_x, and the layer interface, as measured from some reference level, be h_T, h_R, and h_D, respectively, and let $d_{T,R} = h_d - h_{T,R}$.

We note in the cases of practical interest that the elevation angle remains sufficiently small throughout the ray trajectory. Under such a circumstance, the elevation angles $\underset{\sim}{\theta}_T$ at T_x (the take-off angle) and $\underset{\sim}{\theta}_R$ at R_x (the angle of arrival) in the EF system may be approximated by the corresponding angles θ_T and θ_R, respectively, in the actual geometry (see Section A2.2). Similarly, the elevation angle $\underset{\sim}{\theta}_D$ (the grazing angle) in the EF system where the ray hits the layer interface for the first time after it leaves T_x may be approximated by the angle θ_D in the actual geometry.

Further, let the lower and upper atmospheric layers be called Layers I and II, respectively.

The problem to be solved is to determine, for each of the cases (A), (B), and (C), all the possible ray paths that connect T_x to R_x. We will show that this can be reduced to the problem of determining the unknown angles θ_T, θ_R, and θ_D for a given set of link parameters. However, the three equations for them will be found to be nonlinear so that more than one solution for the problem can be obtained. The collection of the acceptable solutions that are picked up from among these general solutions form what we will call the multipath.

However, before proceeding to write down the unified set of equations for cases (A), (B), and (C), a few remarks are in order.

First, we establish a sign convention for the angles. In the following treatment of the problem using the EFM we define the x axis (a reference axis) to be the line in the plane of the ray that runs parallel to the earth's surface and points positively along the direction from T_x toward R_x. Then we define the elevation angle at an arbitrary point on the trajectory as the angle made by the positive tangent at that point according to the standard convention. That is, if the reference axis must be rotated counterclockwise to align it with the positive tangent, the elevation angle is positive, and if the reference axis must be rotated clockwise to align it with the positive tangent, the elevation angle is negative. When the elevation angle at a point on a circular arc is transferred to a central angle formed by the normal to the arc at that point and the vertical radial of the circle, the sign and magnitude of the elevation angle reappear conserved as the central angle if we regard the vertical radial as a new reference axis and assign a magnitude and a sign to the central angle as before. By following this standard method, which is uniformly applicable, we can alleviate the confusing sign-assigning rules used in Ref. 2.

Second, since the ray trajectory within a layer is a circular arc we should be aware of the fact that a statement like "a terminal with a given height lies on a ray trajectory" will, in general, correspond to two different situations where the elevation angle of the ray at the terminal is positive or negative. That this

observation is of importance will become clear when we start writing down the equations that determine the ray trajectory.

Finally, we note that, depending upon the relative sizes of L, d_T, d_R, and L_{II}, it will become possible for a ray that entered the second layer to emerge from it and reenter the original layers, and repeat this meandering n times[4] where n = 0, 1, 2, ... In Figures 1 and 3 the meandering of the ray trajectory across the layer interface is represented by a pair of short vertical dotted lines at a point where the ray crosses the interface. Referring to Figure 1 where only the case of $\theta_R < 0$ is sketched for illustrative purposes, we have for case (B)

$$d_R = R_f(\cos \theta_R - \cos \theta_D)$$

$$d_T = R_f(\cos \theta_T - \cos \theta_D)$$

$$L = R_f(\sin \theta_D - \sin \theta_T) + n \cdot 2(R_f + R) \sin \theta_D + 2R \sin \theta_D$$

$$+ R_f (\sin \theta_D + \sin \theta_R)$$

$$= (2n + 2)(R_f + R) \sin \theta_D + R_f \sin \theta_R - R_f \sin \theta_T$$

$$\tag{1}$$

In the above, $R_f = |R_I|$ and $R = R_{II}$ where R_i, i = I, II, are the radii of curvature $R_i = 10^6/(L_i - 1/a)$ of the ray trajectory in Layers I and II. Note, that Eq. (1) is valid for $\theta_T \gtrless 0$ and $\theta_R \gtrless 0$ so that four combinations of θ_T and θ_R are possible. (These possibilities have also been mentioned in Appendix B of Ref. 3.)

By introducing new variables

$$\xi = \sin \theta_R \quad , \quad \eta = \sin \theta_T \quad , \text{ and } \quad \zeta = \sin \theta_D \quad , \tag{2}$$

Eq. (1) becomes

$$\sqrt{1 - \xi^2} - \sqrt{1 - \zeta^2} = \alpha_1$$
$$\sqrt{1 - \eta^2} - \sqrt{1 - \zeta^2} = \alpha_2$$
$$\xi - \eta + \tau^{-1} \zeta = \alpha_L \quad , \tag{3}$$

---

4. The symbol n used here should not be confused with the refractive index n(r).
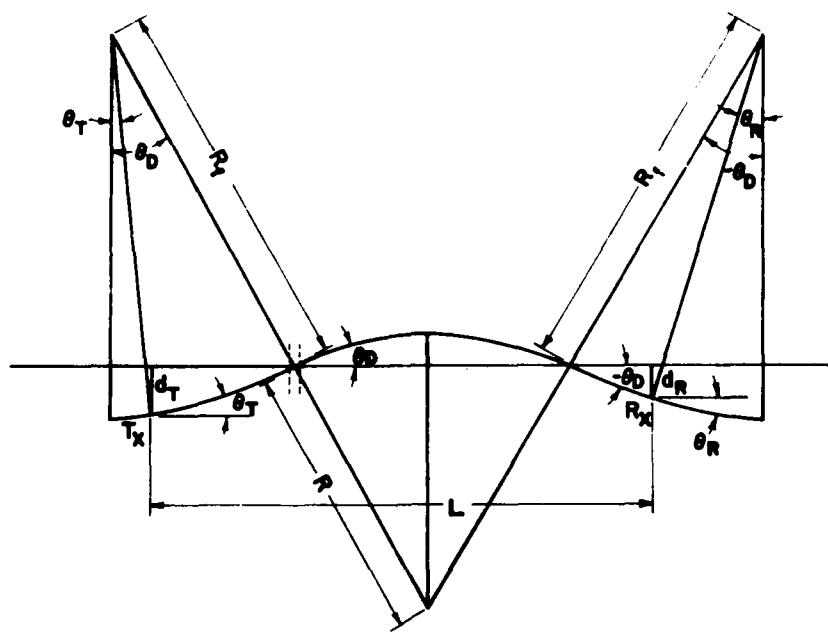
Figure 1. Ray Path for Case (B)

where

$$\alpha_1 = d_R/R_f$$

$$\alpha_2 = d_T/R_f$$

$$\alpha_L = L/R_f$$

$$\alpha_R = R/R_f$$

$$\tau^{-1} = (2n+2)(1 + \alpha_R) \quad . \tag{4}$$

Note that the dimensionless numbers α defined in Eq. (4) are of more physical interest than those numbers introduced in Ref. 2. Combining Eq. (3) with similar equations for cases (A) and (C), we obtain a unified set of equations applicable to all cases,

$$\sqrt{1 - \xi^2} - \sqrt{1 - \zeta^2} = a_1$$

$$\sqrt{1 - \eta^2} - \sqrt{1 - \zeta^2} = a_2$$

$$b\xi + c\eta + d\zeta = \alpha_L \quad , \tag{5}$$

where the values of the constants a_1, ..., d for each case are given in Table 1. (We also included in Table 1 the values of constant d_o which is relevant to the direct paths (see Section 2.1.3).)

Table 1. Values of Constants for Cases (A), (B), and (C)

Constant \ Case	(A)	(B)	(C)
a_1	$-\alpha_1/\alpha_R$	α_1	$-\alpha_1/\alpha_R$
a_2	α_2	α_2	$-\alpha_2/\alpha_R$
b	$-\alpha_R$	1	$-\alpha_R$
c	-1	-1	$+\alpha_R$
d	$\sigma^{-1} = (2n+1)(1+\alpha_R)$	$\tau^{-1} = (2n+2)(1+\alpha_R)$	$-\tau^{-1}$
d_o	$\sigma_o^{-1} = 1 + \alpha_R$	0	0

Having obtained the unified set, we must then solve it. Since, however, the solution procedure for the unknowns is nearly the same, we will discuss only the solution for η as an example.

It will be seen that the equation for η that can be derived from Eq. (5) is of eighth degree. Unfortunately, the theory of equations is of little use in assessing the nature of the roots of such an equation. On the other hand, we see that we do not have to solve Eq. (5) exactly because the practical situation we will be interested in is the one for which both of the conditions $r \approx a$ and $\cos \theta \approx 1$ are applicable.

2.1.2 SMALL-ANGLE APPROXIMATION

Since we have, in general, a series expansion for $\cos \theta$ given by

$$\cos \theta = 1 - \frac{1}{2} \sin^2 \theta - \frac{1 \cdot 1}{2 \cdot 4} \sin^4 \theta - \cdots$$

or equivalently, with $x = \sin \theta$

$$\sqrt{1 - x^2} = 1 - \frac{1}{2} x^2 - \frac{1 \cdot 1}{2 \cdot 4} x^4 - \cdots$$

11

the condition $\cos \theta \approx 1$ which has been mentioned above indicates that the square root terms in Eq. (5) may be approximated by the series form truncated at the second term (the small-angle approximation) yielding

$$\xi^2 - \zeta^2 = -2a_1$$

$$\eta^2 - \zeta^2 = -2a_2$$

$$b\xi + c\eta + d\zeta = \alpha_L \quad . \tag{6}$$

To obtain the equation for η we may proceed as follows: First, from the first two equations we get

$$\xi^2 - \eta^2 = -2(a_1 - a_2) \equiv -2a_- \quad . \tag{7}$$

Next, substituting the expression for ζ obtainable from the third equation into the second and using Eq. (7) we obtain

$$\xi = (M_2 \eta^2 + M_1 \eta + M_0)/2b(c\eta - \alpha_L), \tag{8}$$

where

$$M_2 = d^2 - (b^2 + c^2)$$

$$M_1 = 2\alpha_L c$$

$$M_0 = 2a_2 d^2 + 2a_- b^2 - \alpha_L^2 \quad . \tag{9}$$

Substituting Eq. (8) into Eq. (7) we then obtain a quartic equation given by

$$\sum_0^4 A_i \eta^i = 0 \tag{10}$$

where

$$A_4 = M_2^2 - 4b^2 c^2$$

$$A_3 = 4\alpha_L c(M_2 + 2b^2)$$

12

$$A_2 = 2M_2 M_0 - 4\alpha_L^2 (b^2 - c^2) + 8a_- b^2 c^2$$

$$A_1 = 4\alpha_L c(M_0 - 4a_- b^2)$$

$$A_0 = M_0^2 + 8\alpha_L^2 a_- b^2 \quad . \tag{11}$$

It is to be noted that n = 0 for case (A) is an exception where we have $A_4 = 0$ so that the resulting equation is cubic instead of quartic. This is related to the apparent discontinuity of Eq. (10) that will be discussed in Section 2.1.4.

We think that this represents an appropriate stage at which a closer comparison of Eq. (10) with the similar equation derived according to the RSM should be made. In Ref. 3 Málaga and Parl derive a quartic equation [their Eq. (2.42)] for an unknown $x = \theta_T / \phi$ that is applicable to all conceivable terminal configurations. Rewritten as an equation for θ_T it is given by

$$\sum_0^4 A_i \theta_T^i = 0 \tag{12}$$

where

$$A_4 = a_1^2 - a_2$$

$$A_3 = (2a_1 b_1 - b_2)\phi$$

$$A_2 = (b_1^2 + 2a_1 c_1 - c_2)\phi^2$$

$$A_1 = (2b_1 c_1 - d_2)\phi^3$$

$$A_0 = (c_1^2 - e_2)\phi^4 \quad . \tag{13}$$

In Eq. (13), $\phi = D/R_0$ corresponds to our $\alpha_L = L/R_f$ and the eight constants a_1, b_1, c_1, a_2, b_2, c_2, d_2, and e_2 depend on other constants k_{12}, k_T, k_R, ϵ_T, ϵ_R, R_{eT}, and R_{eR} that are defined in terms of the link parameters. The intended comparison, therefore, requires a more detailed knowledge of these constants. However, considering the fact that Ref. 3 has never been circulated (it was intended only for RADC/EE internal information) it makes little sense to go into detailed discussions of the comparison of Eqs. (10) and (13). Therefore, we will state here simply that the result of a detailed comparison between the coefficients shows that

$$A_i = A_i \delta^4 \quad , \quad i = 0, 1, \ldots, 4$$

where $\delta = a/R_f$. In this way we may conclude that the roots for $\eta = \sin \theta_T$ obtained by the EFM are identical to θ_T obtained by the RSM. This shows that the take-off angles, the acceptable solutions among these roots, found by the two methods are equivalent to the extent that one can regard $\sin \theta_T \approx \theta_T$. A similar statement can be made concerning the angle-of-arrival. It should be noted that included in Eq. (3.12) of Ref. 3 is what they call the LOS path (which is the same as the direct path) corresponding to the cases where both terminals are located in the same layer of the atmosphere. In contrast to this, our Eq. (10) is applicable to the nondirect paths only, that is, to the cases where the ray crosses the layer interface at least once and hence excludes the LOS path. Therefore, strictly speaking, equivalence of Eqs. (10) and (12) extends only up to our nondirect paths. However, the equivalence of the equations for the LOS path in Ref. 3 and the direct path in our work (see Section 2.1.3) can be readily established so that it can still be concluded that the ray-path equations according to the EFM are entirely equivalent to those according to the RSM.

Incidentally, a quartic equation is the highest degree equation that can be solved algebraically. The sign of the discriminant indicates the kinds of roots the equation has. Since the discriminant is a function of the link parameters via the coefficients of the equation we can get some information on the relation of the parameters to the properties of the roots. In practice, however, these parameters enter these relations in such an intertwined manner that no useful information can readily be extracted from these relations.

We note that for a given set of link parameters we can find all the acceptable paths that interfere with the layer interface in the following manner: We consider the solutions to Eq. (6) corresponding to nonnegative integer values of n starting with n = 0 and extending up to a certain maximum which can be seen to exist by examining Eq. (6). For each value of n the four roots of Eq. (6) must be examined, and solutions accepted only if they are both real (that is, the complex-valued roots must be discarded), and also small (that is, very close to zero). The collection of the acceptable solutions of Eq. (6) thus found will constitute the totality of the paths that cross the layer interface.

2.1.3 DIRECT PATH

Although it was not made unmistakably clear when Eq. (5) was first written, it was implicit that it was intended for dealing with only those ray paths that cross the layer interface [interface-crossing (IFC) paths].

For case (B) or (C), when the natural propagation of the waves is not obstructed, there can exist a ray path that is not included in Eq. (5). Such a path that does not cross the layer interface is usually referred to as the direct path.

14

For case (A) there does not seem to be any obvious criterion according to which the direct path can be defined, except for the requirement that it should be a path that crosses the layer interface just once; that is, $n = 0$ for that case. However, it is possible to define the direct path for case (A) in the following way. Namely, of the possible three solutions to Eq. (6) for $n = 0$ of case (A) one can pick up that real solution that will go over, for the fixed link parameters, to the direct path for case (B) in the limit when the height of the layer interface is raised to approach to the height of R_x. We will define the path that corresponds to this solution to the cubic equation as the direct path in conjunction with (or relative to) case (B). [Actually, this path should more properly be regarded as the extension to case (A) of the direct path for case (B).] Similarly, the solution of the cubic equation that goes over to the direct path for case (C) in the limit when the height of the layer interface approaches to that of T_x will be defined as the direct path for case (A) in conjunction with case (C). A fact to be remembered in this definition is that the direct path for case (A) is a solution for $n = 0$ of Eq. (6) for case (A).

As a result of this definition, we can have a unified set of equations for the direct path [see Eq. (14) below] with the understanding, which will often be repeated in what follows, that the appropriate solution for case (A) must be singled out from the three possible solutions. Also, it should be possible to establish the interconnection among our nondirect paths, the conventional nondirect paths [where the direct path is defined only for cases (B) and (C)], and the IFC paths.

With our definition of the direct path, Eq. (14) gives the exact and Eq. (15) the approximate sets of equations for the direct path:

$$\sqrt{1 - \xi^2} - \sqrt{1 - \zeta^2} = a_1$$

$$\sqrt{1 - \eta^2} - \sqrt{1 - \zeta^2} = a_2$$

$$b\xi + c\eta + d_o\zeta = \alpha_L \quad , \tag{14}$$

$$\xi^2 - \zeta^2 = -2a_1$$

$$\eta^2 - \zeta^2 = -2a_2$$

$$b\xi + c\eta + d_o\zeta = \alpha_L \quad . \tag{15}$$

In these equations, the values of a_1, a_2, ..., and d_o, for each case, are listed in Table 1.

The procedure for determining the direct path by solving Eq. (15) is seen to be identical to that for the IFC paths with the replacement of d by d_o.

In cases (B) and (C), however, it will be simpler to solve Eq. (15) anew under the special conditions that apply to these cases; that is, $b = -c$ and $d_o = 0$. This leads to the solution given by:

$$\left.\begin{array}{c} \xi \\ \eta \end{array}\right\} = \pm \frac{\alpha_L}{2b} - \frac{a_- b}{\alpha_L} \quad .$$

With $b = 1$ and $-\alpha_R$ for cases (B) and (C), respectively, we may combine the result as

$$\left.\begin{array}{c} \xi \\ \eta \end{array}\right\} = \mp \frac{L}{2\mathcal{R}} + \frac{e}{L} \quad . \tag{16}$$

In this equation we set

$$e = d_T - d_R$$

and

$$\mathcal{R} = \begin{cases} -R_f = R_I & \text{for case (B)} \\ +R = R_{II} & \text{for case (C)} \end{cases}, \tag{17}$$

where R_I and R_{II} are the radii of curvature of the ray trajectories in Layers I and II, respectively.

In the foregoing, we solved Eqs. (6) and (15), the small-angle approximate versions, for both the nondirect and direct paths, for reasons of consistency.

In contrast, Pickering and DeRosa,[2] in discussing case (B), solved the exact relations for the direct path [in a manner equivalent to solving our Eq. (14)], while solving the approximate relations for the nondirect paths. Since the exact set for the direct path for cases (B) and (C), [Eq. (14)] can readily be solved analytically, it will be of some interest to discuss the solution of Eq. (14).

For cases (B) and (C), Eq. (14) leads to a quadratic equation for ξ or η. The solutions are given by

$$\xi = \frac{1}{2}\left(+ \frac{\alpha_L}{b} \pm \beta \right)$$

$$\eta = \frac{1}{2}\left(- \frac{\alpha_L}{b} \pm \beta \right)$$

$$\beta = |a_-| \sqrt{\left(\frac{2b}{\sqrt{\alpha_L^2 + a_-^2 b^2}} \right)^2 - 1} \qquad (18)$$

where the upper (or lower) signs of ξ and η go together to be consistent with the third of Eq. (14).

We now examine the problem from a geometrical rather than an algebraic viewpoint to see whether or not both possible signs represent acceptable results. Referring to Figure 2 for case (B) for example, we have

$$\sin(\psi - \theta_T) = \sin(\theta_R - \psi) = \frac{t/2}{R_f}$$

where

$$t = \sqrt{L^2 + e^2} \quad .$$

Noting that $\sin \psi = e/t$, we then obtain

$$\theta_{\substack{R \\ T}} = \sin^{-1} \frac{e}{t} \pm \sin^{-1} \frac{t}{2R_f} \quad .$$

From this we get

$$\left. \begin{matrix} \xi \\ \eta \end{matrix} \right\} = \sin \theta_{\substack{R \\ T}} = \frac{e}{t} \cdot \sqrt{1 - \left(\frac{t}{2R_f}\right)^2} \pm \sqrt{1 - \left(\frac{e}{t}\right)^2} \cdot \frac{t}{2R_f} = \frac{e}{2R_f} \sqrt{\left(\frac{2R_f}{t}\right)^2 - 1} \pm \frac{L}{2R_f} , \quad (19)$$

which is seen to coincide with the result in Ref. 2 when their sign convention for θ_R is taken into account. The result given by Eq. (19) agrees with the upper-sign solution of Eq. (18) for case (B). Now, a question remains as to what kind of circumstances would give rise to the lower-sign solution of Eq. (18) for case (B) and whether the solution is physically acceptable.

17
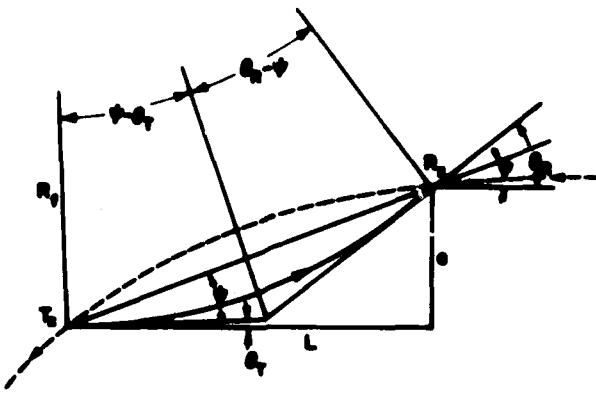
Figure 2. Direct Path for Case (B)

To see this, suppose that we are given a problem in which the wave can travel along the circular arc of radius R_f. If we consider a ray which, after leaving T_x, travels along the dotted circular arc of radius R_f of Figure 2 in the direction indicated by the arrow, the geometrical treatment similar to the above can be shown to lead to the solution:

$$\left.\begin{array}{c} \xi \\ \eta \end{array}\right\} = -\frac{e}{2R_f} \sqrt{\left(\frac{2R_f}{t}\right)^2 - 1} \pm \frac{L}{2R_f} \ . \tag{20}$$

This is identical to the lower-sign solution for case (B) of the exact set, Eq. (18). However, we can readily see that the propagation of the ray from T_x to R_x along the dotted line in the indicated direction is clearly in violation of the conditions for the ray path which we set forth in the beginning. Therefore, we have to reject the solution given by Eq. (20) or the lower-signs of Eq. (18), and will be left with only one set of solutions represented by Eq. (19).

Proceeding analogously we can show that the lower-sign solution of Eq. (18) for case (C) must be discarded also.

Combining the results for cases (B) and (C) we see that the exact set of equations for these cases yields the following acceptable solutions:

$$\left.\begin{array}{c} \xi \\ \eta \end{array}\right\} = \mp \frac{L}{2\mathcal{R}} + \frac{e}{2|\mathcal{R}|} \sqrt{\left(\frac{2\mathcal{R}}{t}\right)^2 - 1} \ . \tag{21}$$

We should note that normally $|2R|/t \gg 1$ so that the second term on the right-hand side of Eq. (21) is approximately equal to e/t which under our assumptions of

18

$r = a$ and $\cos H = 1$ may be regarded equal to e/L. This shows that the exact result, Eq. (21), is practically the same as the approximate one, Eq. (16).

2.1.4 CONNECTION FORMULAS

According to the definition of the direct path given in the previous subsection, Eq. (6) with $n = 0, 1, 2, \ldots$ will provide the complete description of path geometry of the multipath for case A; that is, the direct plus nondirect paths. However, for case (B) or (C) it will not become complete until the equation for the direct path, Eq. (15), is brought in. Although this observation is sufficient for a qualitative argument it is not sufficient for quantitative description because the continuous transition of the multipath phenomenon between cases (A) and (B) or cases (A) and (C) requires a little more precise statement which we might call the connection formulas [see Eqs. (31) and (32) below]. [If we disregard the physical significance attached to the nonnegative integer n and extend its range to include $n = -1$ on purely formal grounds, then Eq. (6) corresponding to this added value of n is seen to coincide with Eq. (15) for cases (B) and (C). Then Eq. (6) with the extended range $n = -1, 0, 1, \ldots$ will describe the entirety of the acceptable paths for cases (B) and (C), in the same way as Eq. (6) with $n = 0, 1, 2, \ldots$ will for case (A).]

To determine the connection formulas, let us consider the transition between cases (A) and (B); that is, the situation where T_x is located in Layer I while R_x sits exactly on the layer interface. Depending upon how we view this, namely, whether we regard this as the limiting case of (A) or (B) in which $d_R \to 0$, we may have to employ the appropriate version of Eq. (6) to analyze it.

However, before dealing with the above problem let us digress a little to examine the special case of (B), called (BS), in which we have $d_T = d_R = d_S$, because it will help us gain some insight into the handling of the transition case problem.

Equation (6) for case (BS) is given by

$$\xi^2 - \zeta^2 = -2\alpha_S$$

$$\eta^2 - \zeta^2 = -2\alpha_S$$

$$\xi - \eta + \tau^{-1}\zeta = \lambda_L \quad , \tag{22}$$

where $\alpha_S = d_S/R_f$. This may be reduced to

$$\eta^2 - \zeta^2 = -2\alpha_S \qquad \qquad \zeta = \tau\left(\alpha_L + \begin{Bmatrix} 0 \\ 2\eta \end{Bmatrix}\right) \tag{23}$$

19

where the upper and lower lines of the second equation correspond to $\xi = +\eta$ and $\xi = -\eta$, respectively. If all four of the solutions are acceptable, we note that the two solutions with $\xi = -\eta$ correspond geometrically to those ray trajectories that are individually symmetrical with respect to the perpendicular line that passes through the midpoint between the terminals (disregarding temporarily the two short dotted vertical lines shown in Figure 3). On the other hand, the two with $\xi = +\eta$ are asymmetrical individually with respect to the perpendicular, but each is the symmetric image of the other with respect to the perpendicular.

By calling the solutions for $\xi = +\eta$ and $\xi = -\eta$ classes (a) and (b), respectively, and labeling the relevant quantities with the corresponding subscript, we obtain the following quadratic equation for each class:

$$\tau^{-2}\,\eta_a^2 + 2\alpha_S\,\tau^{-2} - \alpha_L^2 = 0 \tag{24a}$$

$$(\tau^{-2} - 4)\,\eta_b^2 - 4\alpha_L\,\eta_b + 2\alpha_S\,\tau^{-2} - \alpha_L^2 = 0 \tag{24b}$$

with the solution

$$\eta_{a\,\frac{1}{2}} = \pm\,\tau\alpha_L\,\sqrt{1 - \tau^{-2}\,\frac{2\alpha_S}{\alpha_L^2}} \tag{25a}$$

$$\eta_{b\,\frac{1}{2}} = \frac{2\alpha_L}{\tau^{-2} - 4}\left(1 \pm \frac{\tau^{-1}}{2}\sqrt{1 - (\tau^{-2} - 4)\,\frac{2\alpha_S}{\alpha_L^2}}\right). \tag{25b}$$

Figure 3. Paths for Case (BS)

The condition for the roots of classes (a) and (b) to be real are given by $n_{a,b} \geq n$ where

$$n_{a\atop b} = \frac{1}{2(1 + \alpha_R)}\sqrt{\begin{Bmatrix}0\\4\end{Bmatrix} + \frac{\alpha_L^2}{2\alpha_S}} - 1\ . \tag{26${a\atop b}$}$$

20

Therefore, the necessary condition on the link parameters for the occurrence of a nondirect path is given by $n_{a,b} \geq 0$. Using Eqs. (26a) and (26b), we obtain

$$R_\ell L^2/8 \left[(R_\ell + R)^2 - \begin{Bmatrix} 0 \\ R_\ell^2 \end{Bmatrix} \right] \geq d_S$$

for classes (a) and (b) corresponding to the upper and lower lines, respectively.

When $n_a < 0$ or $n_b < 0$ there will be no real nondirect path for class (a) or (b). On the other hand, when $n_a \geq 0$ or $n_b \geq 0$, additional real solutions may be found corresponding to the positive integer values of $n = 1, 2, \ldots$ up to $\lfloor N_a \rfloor$ or $\lfloor N_b \rfloor$ where the symbol $\lfloor q \rfloor$ denotes the nonnegative integer closest or equal to but not greater than q. Since it can be shown that $n_b - n_a < 1$ we will have the relation $n_a < n_b < (n_a + 1)$ which shows that $\lfloor n_b \rfloor$ can exceed $\lfloor n_a \rfloor$ by unity at the most. The total number of real solutions for $n_a \geq 0$ is given in general by $2(\lfloor n_a \rfloor + 1)$. Using this information, we can easily determine the total number of real nondirect paths for case (BS), which consists of those for classes (a) and (b).

The foregoing shows that in the special case of (BS) the quartic, Eq. (10) can be factored into two quadratic equations thereby enabling us to find the analytic solutions to the original quartic equation in a very simple way.

However, as soon as the condition $d_T = d_R$ is relaxed we lose the symmetry relations $\xi = +\eta$ and $\xi = -\eta$ and the relevant quartic equation can no longer be factored in an obvious manner as was possible for case (BS). We surmise then that we will have to resort to computers to solve the general quartic equation for case (B).

We can now profitably return to our original question: What is the connection between the paths for the limiting case of (A), called case (AI), and those for the limiting case of (B), called case (BI), where T_x is found at the same position in Layer I and R_x sits on the layer interface?

For cases (AI) and (BI) we have $d_R = 0$ so that Eq. (6) becomes

$$\xi^2 - \zeta^2 = 0$$

$$\eta^2 - \zeta^2 = -2a_2$$

$$b\xi + c\eta + d_S = \alpha_L \ . \tag{27}$$

In analogy to case (BS) let us continue to call $\xi = +\zeta$ and $\xi = -\zeta$ classes (a) and (b), respectively. Drawing the trajectories for each of the classes will clarify the geometrical significance. Proceeding as for case (BS), by referring to Table 1,

21

we find the following set of equations applicable to classes (a) and (b) for both cases (AI) and (BI).

$$\eta^2 - \zeta^2 = -2\alpha_2$$

$$\zeta = \kappa(\alpha_L + \eta) \quad , \tag{28}$$

where

$$\kappa_{\substack{a\\b}}^{-1}(n) = d(n) \pm b = \begin{cases} \sigma^{-1} \mp \alpha_R \\ \tau^{-1} \pm 1 \end{cases} = \begin{cases} (2n+1) + (2n + \begin{Bmatrix} 0 \\ 2 \end{Bmatrix} \alpha_R) \equiv \sigma_{\substack{a\\b}}^{-1}(n) & \text{for case (AI)} \\ \left(2n + \begin{Bmatrix} 3 \\ 1 \end{Bmatrix}\right) + (2n+2)\,\alpha_R \equiv \tau_{\substack{a\\b}}^{-1}(n) & \text{for case (BI)} \end{cases}$$

$$\tag{29'}$$

Equation (28) leads to a quadratic equation

$$(\kappa^{-2} - 1)\eta^2 - 2\alpha_L\,\eta + 2\alpha_2\kappa^{-2} - \alpha_L^2 = 0 \tag{30}$$

with solutions

$$\eta_{\substack{1\\2}} = \frac{\alpha_L}{\kappa^{-2} - 1}\left(1 \pm \kappa^{-1}\sqrt{1 - (\kappa^{-2} - 1)\frac{2\alpha_2}{\alpha_L^2}}\right)$$

for η_a and η_b for cases (AI) and (BI) with the appropriate expression for κ taken from Eq. (29).

Here again, for given link parameters the above solutions will be real for such nonnegative integer values of n that $[n_{a,b}] \geq n$ where

$$n_{\substack{a\\b}} = \frac{1}{2(1 + \alpha_R)}\left(\sqrt{1 + \frac{\alpha_L^2}{2\alpha_2}} - \kappa_{\substack{a\\b}}^{-1}(0)\right) \quad .$$

The necessary condition for the occurrence of the nondirect paths, $n_{a,b} \geq 0$, may be expressed as before but will not be repeated here.

This shows that the quartic equation for case (AI) or (BI) obtainable from Eq. (10) is expressible as the product of two quadratic equations (30) for classes (a) and (b) of each case.

From the foregoing analysis we see that the solutions to cases (AI) and (BI) for equal n are not exactly the same; that is, not continuous, as evidenced by the different values of κ^{-1} for these cases. In fact, from Eq. (29) we see that

$$\sigma_b^{-1}(n) = \tau_b^{-1}(n) \qquad \text{for } n = 0, 1, 2, \ldots$$

$$\sigma_a^{-1}(n) = \tau_a^{-1}(n - 1) \quad \text{for } n = 1, 2, 3, \ldots \quad . \tag{31}$$

Here we note for class (a) that the partner for $n = 0$ of case (AI), $\sigma_a^{-1}(0)$, is missing from the collection of τ_a^{-1} for case (BI).

If the direct path has been counted from the beginning in the collection of the acceptable solutions for case (B), then in the limiting situation under consideration we will have the direct path to match up with the solution corresponding to $\sigma_a^{-1}(0)$ such that we will have

$$\begin{array}{l}\text{Solution corresponding} \\[6pt] \text{to } \sigma_a^{-1}(n)\end{array} = \begin{cases} \begin{array}{l}\text{The limit for } d_R \to 0 \text{ of the} \\ \text{direct path for case (B)}\end{array} & \text{for } n = 0 \\[12pt] \begin{array}{l}\text{Solution corresponding} \\ \text{to } \tau_a^{-1}(n - 1)\end{array} & \text{for } n = 1, 2, 3, \ldots \end{cases}$$

$$\tag{32}$$

That is, the cubic equation for $n = 0$ of case (AI) which factors into the product of a linear equation corresponding to $\sigma_a^{-1}(0) = 1$ and a quadratic equation corresponding to $\sigma_b^{-1}(0) = 1 + 2\alpha_R$ will be made to continue to the product of the linear equation for the direct path and a quadratic equation corresponding to $\tau_b^{-1}(0) = 1 + 2\alpha_R$ for case (BI). Thus, the discontinuity existing between the solutions for cases (A) and (B) of Eq. (6) will be remedied properly to achieve continuity by considering for case (B) not only the solutions to Eq. (6) but by augmenting it by direct path.

A discussion analogous to the foregoing can explain the situation in which R_x is situated in Layer II while T_x is found on the layer interface. This may be regarded as a limiting situation of case (A), called case (AII), or as a limiting situation of case (C), called case (CII), and the solution in the multipath phenomenon can be made continuous by introducing the direct path for case (C) into an otherwise apparently discontinuous set of solutions to Eq. (6) for cases (AII) and (CII).

In concluding the subsection let us comment briefly on the connection between the findings on the angles as given in Ref. 3 and in this report (Sections 2.1.1-2.1.4). As we have seen in Section 2.1.2 they are completely equivalent to the

23

extent that we can regard $\sin \theta = \theta$ to be a very good approximation. However, the manner in which our and their findings are presented differ considerably. Therefore, it will be of interest to clarify the connection between the two results. In what follows, we will attempt, to the extent possible, to do that, with the full understanding that Ref. 3 is not available to the reader.

Figures 2-15 and 2-18 of Ref. 3 are reproduced with some modifications in Figure 4. These modifications include the addition of an extra dotted or solid line to the single-lined original curve and attaching arrows, various markings, and numerals for the integers m and n, to facilitate identification. Here, the relation between their m and our n is m = 2n + 1 for case (A) and m = 2n + 2 for cases (B) and (C). The curves in the figure are related to our analysis in the following way:

Consider first Figure 4(b) where the curves in the right and left half-plane correspond to the events in our cases (BS) and (CS), respectively. [Case (CS) is the special configuration of case (C) with equal terminal heights; that is, it is the counterpart of case (BS).] Confining our attention to its right half for the moment we can see that the curves there may be classified into two distinct groups. The first group consists of a family of parabolas that are symmetric with respect to the abscissa and shrink to the origin. The second also consists of a family of diminishing parabolas each of which is symmetric with respect to a line parallel to but a certain distance from the abscissa. Since the abscissa of the figure labels our $d_S = R_f \alpha_S$ it is seen that the parabolas of the first and second groups represent the angle-of-arrival curves corresponding to our Eqs. (24a) and (24b), respectively, in the order of increasing value of n. At the height of the layer interface indicated by the dashed vertical line, the values of the angle of arrival (according to the definition in Ref. 3) for n = 0 for classes (a) and (b) are marked by the symbols x and ● .

In Figure 4(a) where $h_R - h_T \neq 0$, all cases of (A), (B), and (C) occur. For the case of the layer at the height of R_x, the solutions corresponding to classes (a) and (b) of Eq. (30) are marked by x and ● as before. We see that the segment between the markings x and ▲ of the doubly-lined, outermost curve of the figure corresponds to n = 0 in our notation. The various portions of the segment, however, correspond to the value of 1 or 2 in terms of the integer m used in Ref. 3. The inner isolated curve (an island) of the figure contains a segment between x and ▲ that behaves in the same way as in the outermost curve of the figure. The segment corresponds to n = 1. Now, Ref. 3 gives the angle-of-arrival curves for $h_R - h_T$ less than 10 m chosen for Figure 4(a). Inspection of these curves shows that the number of isolated islands, each surrounded by an outer island in succession, increases as $h_R - h_T$ decreases. In the series of diminishing islands that correspond to the values of n = 1, 2, 3, ..., the occurrence of the same general behavior of the curves that was observed for the outermost curve (n = 0)

24
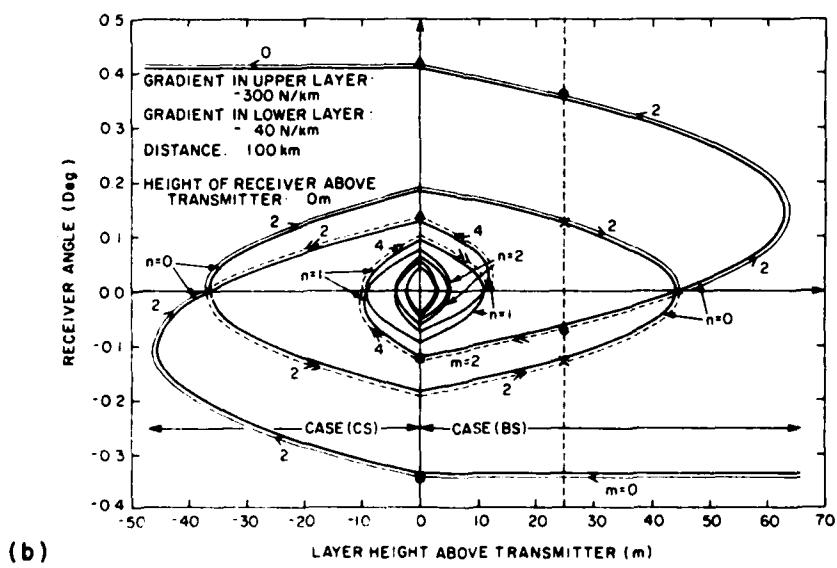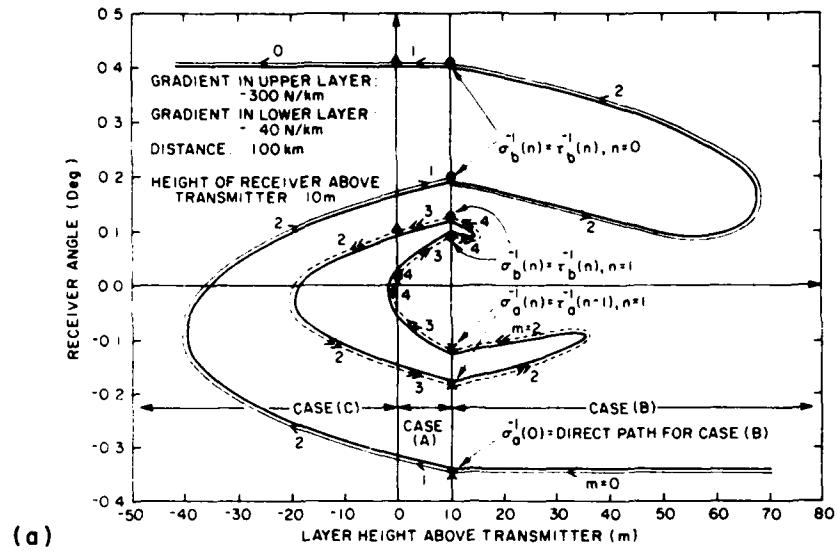
Figure 4. Angle of Arrival (From Ref. 3)

25

is apparent. In the limit of the value of $h_R - h_T$ vanishing, which is the case for Figure 4(b), the islands that previously appeared isolated now have points of contact at various points on the abscissa of the graph. A comparison of Figures 4(a) and 4(b) will show clearly how such contacts occur.

2.2 Time of Arrival

In this section we will present in some detail the result for the time of arrival as derived from the EFM. We will then, as in the previous section, compare the EFM result with the result from the RSM.

2.2.1 NONDIRECT PATH

Figure 1 for case (B), and similar diagrams for cases (A) and (C), show that the height h above the reference level of an arbitrary point on the ray trajectory, where the corresponding central angle (see Section 2.1.1) is $\theta(h)$, is given by

$$h = h_D + \mathcal{R}(\cos\theta - \cos\theta_D) \tag{33}$$

where h_D is the height of the layer interface and

$$\mathcal{R} = \begin{cases} -R_f \\ +R \end{cases} \quad \text{for} \quad h\epsilon \begin{cases} I \\ II \end{cases} \tag{34}$$

Here and in what follows $h\epsilon(I)$, for example, means somewhat loosely that the point with height h is in Layer I.

Now, we recall that the modified refractive index $n_m(r)$ was designated by $\tilde{n}_m(h)$ as a function of h. Renaming it m(h) we see that it may be given by

$$m(h) = m_D + ig(h - h_D) \tag{35}$$

where

$$g = \begin{cases} g_I \\ g_{II} \end{cases} \quad \text{for} \quad h\epsilon \begin{cases} (I) \\ (II). \end{cases}$$

In the above, g_i, $i = I$ and II, are the constant gradients of the modified refractive index for Layers I and II, respectively, and $m_D = m(D)$ is given by

26

$$m_D = m(0) + g_I h_D \quad . \tag{36}$$

Substituting Eqs. (33) and (36) into (35) we obtain

$$m(h) = m_D + g \, \mathcal{R} \, (\cos \theta(h) - \cos \theta_D) \quad .$$

Remembering that

$$\mathcal{R} = -\frac{1}{g}$$

[see the expression for $R_1(P')$ somewhat after Eq. (A26)] the above becomes

$$m(h) = M - \cos \theta(h) \tag{37}$$

where

$$M = m_D + \cos \theta_D \quad .$$

Note that M takes on a different value corresponding to a different multipath, determined as sketched in Section 2.1, for each of cases (A)-(C). To see that M can be represented in different forms let us set h to be $h_{\mathcal{J}}$ where $\mathcal{J}$ can be either T or R. If the elevation angle at $\mathcal{J}_x$ is called $\theta_{\mathcal{J}}$, Eq. (33) gives rise to

$$\cos \theta_D = g \, (h_{\mathcal{J}} - h_D) + \cos \theta_{\mathcal{J}} \quad , \tag{38}$$

which when substituted into Eq. (37) leads to

$$M = m_D + g \, (h_{\mathcal{J}} - h_D) + \cos \theta_{\mathcal{J}} = m_{\mathcal{J}} + \cos \theta_{\mathcal{J}} \quad ,$$

that is,

$$M = m_D + \cos \theta_D = m_T + \cos \theta_T = m_R + \cos \theta_R \tag{39}$$

regardless of T_x or R_x being found in Layer I or II. The equality of the quantity $m + \cos \theta$ at T_x, R_x, and at the point where the path crosses the layer interface as expressed by Eq. (39) is of wider applicability. That it is actually equivalent, under the small angle approximation, to Snell's law can be seen as follows: In the EF system, Snell's law is given by

27

$$m(h) \cos \theta(h) = const$$

along the ray path. Rewriting the left-hand side as

$$[m(h) + \cos \theta(h)] + [m(h) - 1] \cos \theta(h) - m(h)$$

Snell's law becomes

$$m(h) + \cos \theta(h) \approx const$$

along the ray path under the assumption that $m(h) \approx 1$. We see that what is shown in Eq. (39) happens to display the approximate constancy along the ray trajectory of $m + \cos \theta$ at the three special points on it.

To calculate the transit time for the wave to travel from T_x to R_x, it will prove instructive to express the terminal separation L and the curved length S of the path as integrals.

Thus, consider the expression for L, Eq. (1), for case (B) as an example. We may write

$$L = \left\{ \int_{\theta_T}^{\theta_D} R_f + n \left[\int_{\theta_D}^{-\theta_D} (-R) + \int_{-\theta_D}^{\theta_D} R_f \right] + \int_{\theta_D}^{-\theta_D} (-R) + \int_{-\theta_D}^{\theta_R} R_F \right\} \cos \theta \, d\theta$$

$$= - \int_{T_x \to R_x} \mathscr{R} \cos \theta \, d\theta$$

where the integration over θ is carried out from T_x to R_x along the ray trajectory. In so doing we noted that θ increases in Layer I whereas it decreases in Layer II. It will be seen that the last form for L is valid universally for cases (A)-(C).

By comparing the expressions with another one for L [see the third of Eq. (5)]

$$L = R_f (b \sin \theta_R + c \sin \theta_T + d \sin \theta_D) \tag{40}$$

we can see that the values of the coefficients b and c as listed in Table 1 can also be identified with

$$b = \left(- \frac{\mathcal{R}}{R_f} \right) \Bigg|^{R_x}$$

$$c = \left(- \frac{\mathcal{R}}{R_f} \right) \Bigg|_{T_x}$$

whereas the values of the coefficient d do not lend themselves to a simple expression like the ones in the above.

In a similar manner it can be shown that the geometrical length S of the path between T_x and R_x may be given by

$$S = - \int_{T_x \to R_x} \mathcal{R} \, d\theta = R_f (b\theta_R + c\theta_T + d\theta_D) \quad .$$

Returning to the calculation of the transit time τ for the link we see that it is given by

$$\tau = - \int_{T_x \to R_x} \mathcal{R} \, d\theta / [c_o / \overline{m}(\theta)]$$

where $\overline{m}(\theta) \equiv m(h)$ is given by Eq. (37) and c_o is the velocity of light in vacuo. Therefore, we have

$$\tau = \frac{1}{c_o} \left[M \int_{T_x \to R_x} (-\mathcal{R}) \, d\theta - \int_{T_x \to R_x} (-\mathcal{R}) \cos \theta \, d\theta \right] = \frac{1}{c_o} (MS - L)$$

$$= \frac{R_f}{c_o} \left[b(M\theta_R - \sin \theta_R) + c(M\theta_T - \sin \theta_T) + d(M\theta_D - \sin \theta_D) \right] \quad . \tag{41}$$

At this point we would like to compare the above results with those found in Ref. 3. There, the terminal separation D and the transit time τ_{RS} are shown to be given by

29

$$D = m(R_{e1} - R_{e2})\theta_B - R_{eR}\theta_R - R_{eT}\theta_T$$

$$c\tau_{RS} = m(R_{e1} - R_{e2})\sin\theta_B - R_{eR}\cos\theta_B\tan\theta_R - R_{eT}\cos\theta_B\tan\theta_T$$

where c, the velocity of propagation, represents the value at the height of the layer interface. In the above, m = 0, 1, 2, ... denotes the number of crossing of the layer interface by the ray; R_{eT} and R_{eR} are the equivalent earth radii corresponding to the layer of atmosphere (R_{e1} for Layer I and R_{e2} for Layer II) in which T_x and R_x, respectively, may be found; θ_T, θ_B, and θ_R are the angles of take-off, grazing, and arrival, respectively.

Comparing Eqs. (40) and (41) with the expressions for D and $c\tau_{RS}$ given in the foregoing we notice that they are parallel in the sense that the repeated appearance of the same coefficients b, c, and d in the two equations of our set are copied by the appearance of the same coefficients $m(R_{e1} - R_{e2})$, $-R_{eR}$, and $-R_{eT}$ in the two equations of their set. To be noted also is the appearance of θ in D at the places where $\sin\theta$ appears in L. This is, of course, a reflection of the fact that roles of the ray trajectory and the layer interface are interchanged in the EF and RS systems (see Appendix B).

To compare the results in more detail, we note the following: First, our R_f and R correspond to their R_{e1} and $-R_{e2}$, respectively. Next, our θ_T and θ_R correspond to their θ_T and $-\theta_R$, respectively, while our θ_D corresponds to their θ_B for cases (A) and (B) and to $-\theta_B$ for case (C). Therefore, our $R_f d \sin\theta_D = R_f(2n + 1)(1 + \alpha_R)\sin\theta_D$ for case (A) and $R_f d \sin\theta_D = \pm R_f(2n + 2)$ $(1 + \alpha_R)\sin\theta_D$ for cases (B) and (C), n = 0, 1, 2, ... correspond to their $m(R_{e1} - R_{e2})\theta_B$ for m = 1, 3, 5, ... and m = 2, 4, 6, ..., respectively. All combined, it shows that our L given by Eq. (40) is approximately equal to their D on the condition that $\sin\theta \approx \theta$.

What should be of more direct interest to us is to see whether our transit time τ and their τ_{RS} are equivalent. Numerically they cannot be equal, of course, because they are defined relative to different values of propagation velocity c_o and c. A direct comparison will become possible when the transit times are computed relative to the same velocity of propagation. Thus, for example, our τ should be compared with the quantity $\tau_{RS}(c/c_o)$ because they both refer to the same velocity c_o. In other words, we should examine whether the distances $c_o\tau$ and $c\tau_{RS}$ are equal. That this is essentially the case can be seen by re-expressing the three factors of the same form $M\theta - \sin\theta$ that appear in Eq. (41) and comparing the result with the expression for $c\tau_{RS}$ given in Ref. 3. Now, using Eq. (39) we have for the first factor $M\theta_R - \sin\theta_R \approx (m_D + \cos\theta_D)\sin\theta_R - \sin\theta_R \approx \cos\theta_D\tan\theta_R$,

30

and similarly for the second factor, while for the third factor, we have $\approx (M - 1) \sin \theta_D \approx \sin \theta_D$. With the above we see that $c_o \tau$ agrees with $c \tau_{RS}$ showing that the time of arrival results by the EFM and RSM are essentially equivalent on the level of approximation we are interested in. In deriving the above result we noted that $m_D \approx 1$ and $\theta \approx \sin \theta \approx \tan \theta$ are valid for $r \approx a$ and $\cos \theta \approx 1$, respectively.

If we define the time delay as the transit time relative to that in vacuo, then it is given by

$$\tau - \frac{L}{c_o} = \frac{1}{c_o} (MS - 2L) \tag{42}$$

The corresponding quantity $\tau_{RS} - D/c$ is defined as the relative delay in Ref. 3. That $\tau - L/c_o \geq 0$ and $\tau_{RS} - D/c \leq 0$ can naturally be understood in terms of the nature of the EFM and RSM.

At this point we would like to make some comments on the relative delay diagrams in Ref. 3, especially in conjunction with the corresponding angle-of-arrival diagrams. Figures 2-25 and 2-28 of Ref. 3 that give the relative delay for the paths whose angles of arrival are shown in their Figures 2-15 and 2-18, and have been discussed in Section 2.1.4, as our Figures 4(a) and 4(b), are reproduced here as Figures 5(a) and 5(b).

First, let us consider Figure 5(b). We see that the diagram consists of a stack of figure $\times$, one piled on top of another. It can be seen that the bottom section of the stack, shown in double lines, corresponds to the double-lined curve in Figure 4(b). The stacking is due to the repetition of the basic pattern of the figure for n = 0 in the figures for n = 1, 2, 3, ..., which corresponds to the similar repetition observed in Figure 4.

Consider the time delay for paths with n = 0 at some positive layer height in Figure 5(b). Figure 4(b) shows that there are two paths (marked by x) belonging to class (a) and two paths (marked by ●) belonging to class (b) of case (BS). Because the paths of class (a) are symmetric to each other, (see Figure 3), their relative delays are identical; they correspond to one and the same point of the figure. [In Figure 5(b), however, we deliberately represented them as separated.] The same applies to the curves for n = 1, 2, 3, ... of Figure 5(b).

In Figure 5(b) a situation analogous to Figure 5(a) takes place. The difference between the two is that the nonzero value of $h_R - h_T$ in Figure 5(a) results in the spacings between the successive tiers in the stacking structure. In the limit of a vanishing value of $h_R - h_T$ these spacings reduce to zero to produce Figure 5(b).

31
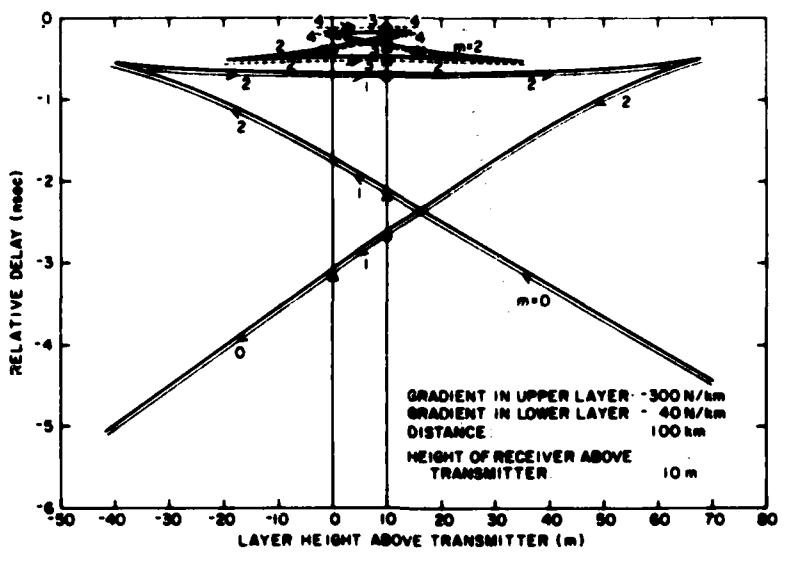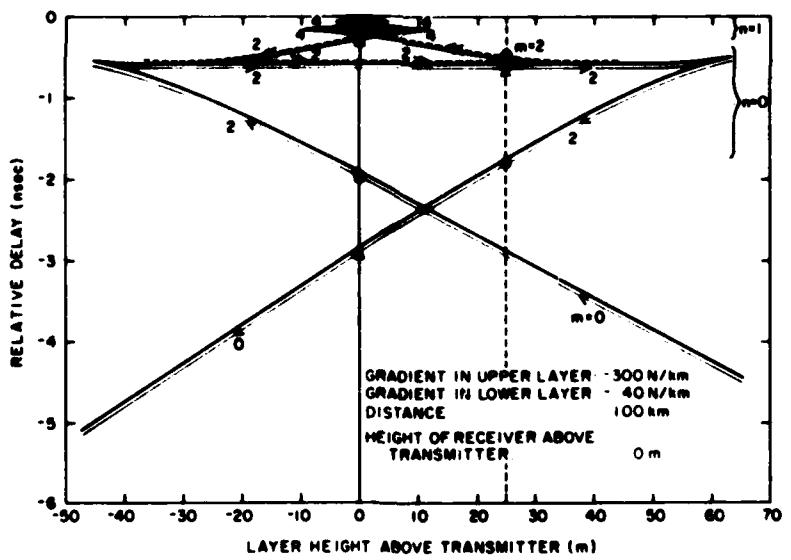
Figure 5. Relative Delay (From Ref. 3)

2.2.2 DIRECT PATH

The expression for the transit time τ_d for the direct path is given by

$$\tau_d = \frac{1}{c_o} (M_d S_d - L)$$

where M_d and S_d are the quantities M and S corresponding to the direct path.
The time delay for the direct path analogous to Eq. (42) is given by

$$\tau_d - \frac{L}{c_o} = \frac{1}{c_o} (M_d S_d - 2L) \tag{43}$$

If the experimental circumstances warrant it, one may be interested in defining the time of arrival of a nondirect path as the transit time relative to that for the direct path. Then the time of arrival $\bar{\tau}$ is given by

$$\bar{\tau} = \tau - \tau_d = \frac{1}{c_o} (MS - M_d S_d) \tag{44}$$

2.3 Amplitude Factor

In this section we will find the power (or intensity) factor, and from it the amplitude factor, associated with a ray as it is received at R_x. The concept of intensity emerges as a result of the assumption that the energy which was initially confined to a narrow bundle of rays that emanates from T_x, and centered around the ray in question, continues to be confined within that same bundle throughout the propagation; the increase and decrease in the intensity of a ray occur corresponding to the contraction and expansion, respectively, of such a bundle.

Consider a small bundle of rays centered around a ray with take-off angle θ_T and angular extents of $\delta\theta_T$ and $\delta\phi$ in the vertical and azimuthal planes, respectively. If the cross-section and the intensity of the bundle are $\delta A(1)$ and $I(1)$ at a point with unit horizontal distance from T_x and the corresponding quantities are $\delta A(L)$ and $I(L)$ at R_x, then we have $\delta A(1)I(1) = \delta A(L)I(L)$ according to the above assumption. When the elevation angle remains small throughout the ray path it can be shown that

$$\delta A(1) \approx \delta\theta_T \cdot \delta\phi \cdot \cos\theta_T$$

$$\delta A(L) \approx |\delta L \cdot L\delta\phi \cdot \sin\theta_R|$$

33

where δL is the horizontal extent of the bundle at R_x. Then in the limit of vanishing cross-section of the bundle we obtain the power factor $\mathscr{P}$ given by

$$\mathscr{P} = \lim \frac{I(L)}{I(1)} = \lim \frac{\delta A(1)}{\delta A(L)} \approx \lim \left| \frac{\cos \theta_T \; \delta \theta_T}{L \sin \theta_R \; dL} \right| = \left| \frac{\partial \eta / \partial L}{L \xi} \right| \tag{45}$$

The amplitude factor α is then defined by

$$\alpha = \sqrt{\mathscr{P}} \; . \tag{46}$$

The corresponding factors for the direct path are

$$\mathscr{P}_d = \lim \frac{I_d(L)}{I_d(1)} \approx \left| \frac{\partial \eta_d / \partial L}{L \xi_d} \right| \quad ,$$

$$\alpha_d = \sqrt{\mathscr{P}_d} \; , \tag{47}$$

where the subscript d refers to the direct path.

If we take the ratio of $\mathscr{P}$ to $\mathscr{P}_d$, we obtain a factor that approximately represents the power of a nondirect ray relative to that for the direct ray. It is given by

$$\overline{\mathscr{P}} = \lim \frac{I(L)}{I_d(L)} \approx \frac{\mathscr{P}}{\mathscr{P}_d} \approx \left| \frac{\partial \eta / \partial L}{\xi} \cdot \frac{\xi_d}{\partial \eta_d / \partial L} \right| \tag{48}$$

on the understanding that the intensities $I_d(1)$ of the direct path and $I(1)$ of a nondirect path at a unit distance from T_x are very nearly equal to each other.

When the free-space propagation, instead of the direct path, is chosen as the reference, the power factor $\mathscr{P}_o$ corresponding to Eq. (47) is given by

$$\mathscr{P}_o = \lim \frac{I_o(L)}{I_o(1)} = \lim \frac{\delta A(1)}{\delta A(L)} = \frac{1}{R^2} \approx \frac{1}{L^2}$$

where the subscript o refers to the free-space and R stands for the slant distance from T_x to R_x. The power factor $\overline{\mathscr{P}}_o$ relative to the free-space intensity is given by

34

$$\overline{\mathscr{P}}_o = \lim \frac{I(L)}{I_o(L)} \approx \frac{\mathscr{P}}{\mathscr{P}_o} \approx \left| \frac{L \partial \eta / \partial L}{\xi} \right| \tag{49}$$

where again we assume that $I(1) \approx I_o(1)$. This is the power factor employed in Ref. 3.

We note that the power factors obtained by the EFM and RSM should be equivalent since they are determined in terms of various angles of a ray path, as shown in the foregoing, that are found to be essentially identical (see Section 2). However, there is one area to which Ref. 3 directed a special attention while Ref. 2 did not touch upon it at all; the intensity near the caustics. We observe that the authors of Ref. 3 discarded the RSM which they had followed consistently up to this point and opted to employ the EFM.

As is well known, the ray theory that is adopted in this report as well as in Refs. 2 and 3 is valid only under certain conditions. In particular, the intensity near the caustics due to the ray theory is in error in the sense that it grows as one approaches a caustic and becomes infinite at the caustic. The standard method of correcting for the errors is to examine the asymptotic solutions near the caustic of the wave equation and compare them with the ray-theory solutions. This has been carried out in Ref. 3, obtaining the necessary corrections to the ray-theory results near and at the caustics. Since their work seems to be sufficiently detailed and accurate, we will not attempt to add anything more to it. We might remark, however, that it would have been awkward and perhaps rather difficult to achieve the same results had they continued to operate in the RS system.

2.3.1 SMALL-ANGLE APPROXIMATION

This is the approximation in which the nondirect and the direct paths are determined by Eqs. (6) and (15), respectively.

Evaluating $\mathscr{P}$ as shown in Eq. (45) by using Eq. (6) we find that

$$\mathscr{P} = \frac{1}{LR_f} \left| \frac{\zeta}{b\eta\zeta + c\zeta\xi + d\xi\eta} \right| . \tag{50}$$

The corresponding expression for $\mathscr{P}_d$ is obtainable from this expression by the substitution $d \to d_o$ and $\xi \to \xi_d = \sin \theta_R^d$, and so on.

Therefore, the amplitude factor $\overline{a} \approx (\mathscr{P}/\mathscr{P}_d)^{1/2}$ can be calculated as soon as ξ, η, and ζ for the nondirect and direct paths are found by solving Eqs. (6) and (15), respectively.

For the direct path for cases (B) and (C) [but not for case (A)] where special conditions $d_o = 0$ and $b = -c$ hold, the expression within the absolute-value sign of Eq. (50) reduces to $a_L^{-1} = R_f/L$ so that we obtain $\mathcal{P}_d = L^{-2}$. This shows that $\mathcal{P}_d$ is approximately equal to $\mathcal{P}_o$, establishing the corresponding equality between the relative power factor $\overline{\mathcal{P}}$ in this report and $\overline{\mathcal{P}_o}$ employed in Ref. 3.

2.3.2 EXACT RESULT

It may be recalled that in Ref. 2 the amplitude factor $\bar{a}$ was calculated for case (B) by employing the approximate solution for the nondirect path and the exact one for the direct path. This apparent nonuniformity should not be a source of any special concern since our assumptions that $r \approx a$ and $\cos \theta \approx 1$ for the ray path will guarantee that the exact and the approximate solutions for the path are practically the same after all. [See the end of Section 2.1.3.]

Nonetheless, for the sake of completeness we will give here the expression for $\mathcal{P}$ derivable from the exact set of Eq. (5). It is given by

$$\mathcal{P} = \frac{1}{LR_f} \left| \frac{\zeta \sqrt{1 - \eta^2}}{b\eta\zeta \sqrt{1 - \xi^2} + c\zeta\xi \sqrt{1 - \eta^2} + d\xi\eta \sqrt{1 - \zeta^2}} \right| .$$

This expression for $\mathcal{P}$ goes over to that in Eq. (50) when the square-root terms are approximated by unity. The exact expression for $\mathcal{P}_d$ may be obtained from the above by the method mentioned in the previous section.

3. CONCLUSION

In this report the two-layer model of the line-of-sight refractive multipath propagation for microwave links has been examined in accordance with the ray theory.

To describe the phenomenon we employed the earth-flattening coordinate system. The result obtained was compared with the corresponding work found by the workers of Signatron, Inc., who adopted the ray-straightening system. Specifically, the angles of take-off and arrival, the time of arrival, and the amplitude factor were examined in detail.

From the purely theoretical point of view, the results for these quantities should not depend on which of the two methods is used. However, the equivalence of the results is not self-evident until it is shown in concrete terms.

It was shown explicitly in this report that the relevant angles, the time of arrival, and the amplitude factor determined by the earth-flattening and ray-straightening methods are in fact essentially equivalent.

36

A1. RAY THEORY IN GENERAL

We will summarize here some well known pertinent results of ray theory.
Given a linear homogeneous partial differential equation

$$f(\nabla, \partial_t)\psi = 0 \quad , \tag{A1}$$

where ∇ is the gradient operator and $\partial_t = \partial/\partial_t$, we get a primary solution of the
form

$$\psi = g(\Theta) \quad ,$$

$$\Theta = \underset{\sim}{a} \cdot \underset{\sim}{x} + a_4 t \tag{A2}$$

with vectors $\underset{\sim}{a} = (a_1, a_2, a_3)$ and $\underset{\sim}{x} = (x_1, x_2, x_3)$, where the coefficients a_i satisfy

$$f(\underset{\sim}{a}, a_4) = 0 \quad .$$

The solution given above also satisfies the so-called equation of characteristics of
the original differential equation defined by

$$f(\underline{\nabla}\psi, \partial_t\psi) = 0 \quad . \tag{A.3}$$

If we specialize to the function

$$f(\underline{b}, b_4) = \underline{b}^2 - b_4^2 / c(\underline{x})$$

we obtain

$$f(\underline{\nabla}, \partial_t)\psi = \nabla^2\psi - \frac{1}{c^2}\partial_t^2\psi = 0 \tag{A4}$$

which represents the scalar wave equation when $c(\underline{x})$ is the speed of propagation at the point $\underline{x}$. The primary solution to this equation may be given by Eq. (A2) with

$$\Theta = \underline{a} \cdot \underline{x} - c_o t$$

where $\underline{a} = \underline{d}/|\underline{d}|$ with the direction cosine vector $\underline{d} = (d_1, d_2, d_3)$, and c_o is the speed of propagation in the empty space. When a more general form for Θ,

$$\Theta = S(\underline{x}) - c_o t \tag{A5}$$

is considered, the equation of characteristics becomes

$$(\underline{\nabla}S)^2 = n^2 \tag{A6}$$

where $n = c_o/c$ is the refractive index. This equation is commonly referred to as the eikonal equation, and is of fundamental importance, leading to the concept of rays. Because of the choice made for Θ in Eq. (A5) it will be seen that the function $\psi = g(S(\underline{x}) - c_o t)$ constructed in terms of the exact solution to the eikonal equation cannot satisfy the original differential equation, that is, the wave equation. Noting first that the solutions in terms of sinusoidal motion is our basic interest and second that the amplitude of the oscillation should be introduced as an unknown function of spatial coordinates, we are led to consider the solution to Eq. (A4) given in the form

$$\psi = A(\underline{x}) \exp[-i\omega\Theta(\underline{x}, t)/c_o] = A(\underline{x}) \exp[i\omega t - ikS(\underline{x})]$$

where $k = \omega/c_o$. Substituting the above into Eq. (A4) and separating the real and imaginary parts we obtain

$$(\nabla S)^2 - n^2 - \frac{\nabla^2 A}{k^2 A} = 0$$

$$\nabla^2 S + \frac{2 \nabla A \cdot \nabla S}{A} = 0 \quad . \tag{A7}$$

For S to be a solution of the eikonal equation the last term of the first equation
must be zero which means that the frequency must be infinitely large. When S is
a solution to the eikonal equation it will serve as a good approximation to the solu-
tion to the wave equation provided that the second term in the second of Eqs. (A7)
is small in comparison to the first. Note, however, that it is not sufficient to say
that k must be large. We have to specify how large k must be relative to the
physical conditions of the problem under consideration. The condition we are
looking for can be found through order of magnitude considerations, and may be
stated as follows:

> A solution to the eikonal equation will serve as a good approximation
> to the phase function in the solution to the wave equation if the frac-
> tional change in the velocity gradient over a wavelength is small
> compared with the velocity gradient itself.

Returning to the question of how to construct the solution to the eikonal equation,
we can show that it is recognizable as a problem of finding a function with a pre-
scribed magnitude, but not direction, of the gradient. It has been known that the
solution leads to the concept of the rays and the wavefront, giving rise to the
vector form of the ray equation for the general case which reduces to simpler forms
for certain special classes of the refractive index. Moreover, it is known that
these ray equations can also be derived from Fermat's principle,

$$\delta \int_1^2 n\,dl = 0 \quad ,$$

where dl is the line element of the ray trajectory, as follows:

(1) General case: $n = n(\underset{\sim}{x})$:

Representing the ray path by $\underset{\sim}{x} = \underset{\sim}{x}(s)$ with a parameter s, we get a line
element given by $dl = \sqrt{\underset{\sim}{x}'(s)^2}\,ds$. Then Fermat's principle is cast into

$$\delta \int_1^2 L[\underset{\sim}{x}(s),\ \underset{\sim}{x}'(s)]\,ds = 0$$

with the Lagrangian $L = n[\underline{x}(s)] \sqrt{\underline{x}'(s)^2}$. The Euler equation corresponding to this leads to the vector form of the ray equation given by

$$\frac{d}{dl} \left(n \frac{d\underline{x}}{dl} \right) = \underline{\nabla} n \quad . \tag{A8}$$

(2) The gradient of n is always in the radial direction:

This corresponds to the case where n is spherically stratified: $n = n(r)$, $r = |\underline{x}|$. If at a point on the ray trajectory its local elevation angle is θ and its position vector makes an angle ϕ with a reference direction through the center, we have $dl = \sqrt{1 + (r\phi')^2} \, dr$ and $L[\phi(r), \phi'(r)] = n(r) \sqrt{1 + (r\phi')^2}$ so that the resulting Euler equation reads

$$rn \cos \theta = \text{const} \quad . \tag{A9}$$

(3) The gradient of n is constant in direction:

Describing n as n(h) in terms of the rectangular coordinates (h, s) we get $dl = \sqrt{1 + s'^2} \, dh$ and $L[s(h), s'(h)] = n(h) \sqrt{1 + s'^2}$. The Euler equation is given by

$$n \cos \theta = \text{const} \quad . \tag{A10}$$

This relation is generally called Snell's law. Because of its relation to Eq. (A10) the relation expressed in Eq. (A8) is usually referred to as the generalized form of Snell's law. We might mention that the name "Snell's law" is frequently applied also to the relation given by Eq. (A9), although some authors may prefer to call it the Bouguer[5] formula.

A2. APPLICATION OF RAY THEORY TO A SPHERICALLY STRATIFIED ATMOSPHERE

The two-layer model of LOS refractive multipath that we want to investigate assumes a spherically stratified atmosphere $n = n(r)$ in a spherical coordinate system having its origin at the earth's center. Then the relation given by Eq. (A9) prevails in the plane that includes the ray trajectory. In this section we will first examine certain aspects of the LOS propagation over the spherical earth for a general spherically stratified atmosphere. Then the same situation will be discussed from the viewpoint of the EFM and the RSM. These results will finally be

---

5. See, for example, Born, M. and Wolf, E. (1965) Principles of Optics, Pergamon Press, New York, p. 123.

specialized to the case of practical interest where the gradient of the refractive index is constant and the transmitter and the receiver are found near the earth's surface. Figure A1 depicts schematically what happens in each of three situations mentioned above. Figure A1(a) shows the propagation of waves in the real world, that is, over a spherical earth, while Figures A1(b) and A1(c) sketch the same event as seen in the EF and RS frame of references.

A2.1 Propagation Over a Spherical Earth

Referring to Figure A1(a) consider a ray which, starting from a point P_1 with polar coordinates $(r_1, \pi/2)$, propagates through a spherically stratified atmosphere $n = n(r)$ and passes through another point P with coordinates $(r, \bar{\phi})$. When the geometrical relation

$$d\phi = \frac{dr \cot \theta}{r} \quad ,$$

where $\phi = \pi/2 - \bar{\phi}$ and θ is the local elevation angle, is combined with the ray path equation for this case [compare with Eq. (A9)]

$$r n \cos \theta = A$$

we obtain the following differential equation for ϕ:

$$\phi'(r) = \frac{\cot \theta}{r} = \frac{A}{r \sqrt{(rn)^2 - A^2}} \quad . \tag{A11}$$

From this equation we obtain the solution

$$\phi(r) = A \int_{r_1}^{r} \frac{dr}{r \sqrt{(rn)^2 - A^2}}$$

as well as the relation

$$\phi''(r) = -A \frac{2(rn)^2 - A^2 + r^3 nn'}{r^2 [(rn)^2 - A^2]^{3/2}} \quad . \tag{A12}$$

41
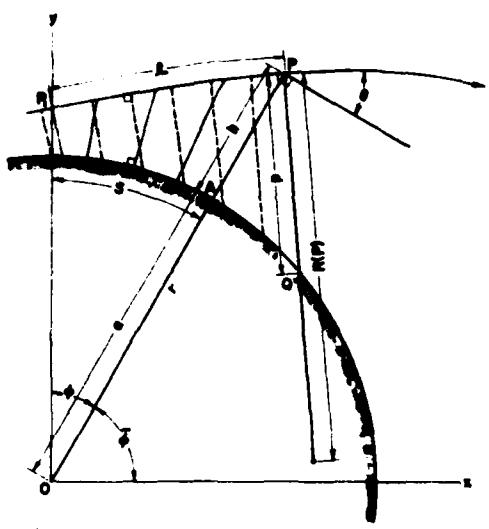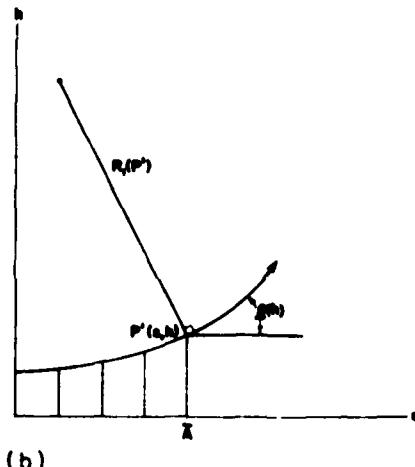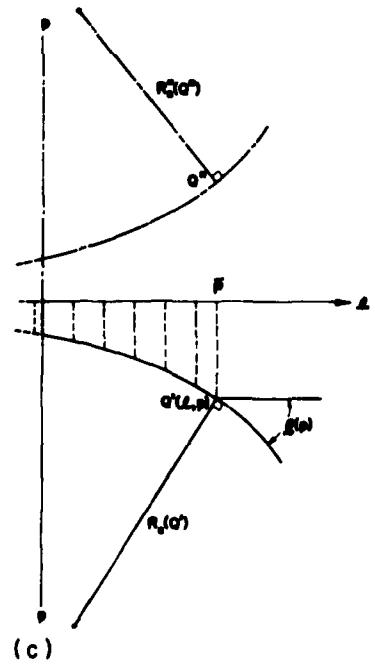
Figure A1. (a) The Actual, (b) Earth-Flattening, and (c) Ray-Straightening Systems

Next, let us define the radius of curvature $R(P)$ at a point P on the ray trajectory, as expressed by $y = y(x)$, by

$$R(P) = - \frac{[1 + y'(x)^2]^{3/2}}{y''(x)}$$

with a minus sign in front. It follows from this definition that the radius of curvature so defined is an algebraic quantity such that it will be <0 (or >0) for a trajectory which is concave up- (or down-) ward. In terms of the polar coordinates $(r, \bar{\phi} = \pi/2 - \phi)$ it becomes

$$R(P) = + \frac{[1 + r^2 \phi'(r)^2]^{3/2}}{2\phi'(r) + r\phi''(r) + r^2 \phi'(r)^3}$$

which on substitution of Eqs. (A11) and (A12) gives rise to[6]

$$R(P) = - \frac{rn^2}{An'} = - \frac{1}{n' \cos\theta/n} \ . \tag{A13}$$

A2.2 Earth-Flattening Transformation

The trajectory of the ray in the earth-flattening coordinate system can be found in the following way. Imagine an observer who moves along the earth's surface and measures the distance traveled s and the height above the ground h of the ray trajectory. Based on these data, construct a rectangular coordinate system (s, h). Then the curve which describes the loci of h as a function of s, that is, $h = h(s)$, represents the ray trajectory in the EF system. Analytically, the EF transformation is characterized by the relations as given below:

$$s = a\phi$$

$$h = r - a \ . \tag{A14}$$

The transformed ray trajectory in the EF system is sketched in Figure A1(b) in which points A and P of the actual configuration are mapped to points $\bar{A}$ and P',

---

6. This relation was derived geometrically in Millington, G. (1957) The concept of the equivalent radius of the earth tropospheric propagation, Marconi Rev. 20(No. 126):79-93.

43

respectively, where the point P' has the coordinates (s, h). The radius of curvature $R_1(P')$ at P' of the transformed trajectory is given, in accordance with the sign convention adopted earlier, by

$$R_1(P') = - \frac{\left[1 + h'(s)^2\right]^{3/2}}{h''(s)} \quad .$$

Noting that

$$h'(s) = \frac{dh/dr}{ds/dr} = \frac{1}{a\phi'(r)}$$

$$h''(s) = \frac{d}{ds}\frac{dh}{ds} = - \frac{\phi''(r)}{a^2\phi'(r)^3} \tag{A15}$$

and using Eqs. (A11) and (A12) we obtain

$$R_1(P') = + \frac{\left[1 + a^2\phi'(r)^2\right]^{3/2}}{a\phi''(r)} = - \frac{r^2\left[1 - \xi^2(1 - a^2/r^2)\right]^{3/2}}{a\xi(2 - \xi^2 + rn'/n)} \quad . \tag{A16}$$

where

$$\xi(r) = A/rn(r) = \cos\theta(r) \quad .$$

At this point we want to make a few remarks regarding Eq. (A16). By substituting $n' = rn^2/AR(P)$ from Eq. (A13) into Eq. (A16) we may express $1/R_1(P')$ in the form

$$\frac{1}{R_1(P')} - \frac{1}{\infty} = \frac{1}{R(P)v_P(r)} - \frac{1}{av_a(r)} \quad ,$$

where

$$v_P(r) = \frac{r}{a}\left[1 - \xi^2(1 - a^2/r^2)\right]^{3/2}$$

$$v_a(r) = \frac{r^2\left[1 - \xi^2(1 - a^2/r^2)\right]^{3/2}}{a^2\xi(2 - \xi^2)} \quad .$$

44

In the case of practical interest where $r \approx a$ and $\cos \theta \approx 1$ throughout the ray trajectory we further note the following.

First, $v_P(r) \approx 1$ and $v_a(r) \approx 1$ under these conditions so that the above relation among the curvatures simplifies to

$$\frac{1}{R_1(P')} - \frac{1}{\infty} \approx \frac{1}{R(P)} - \frac{1}{a} \quad . \tag{A17}$$

The relation shows that the relative curvature between the ray trajectory and the earth's surface taken at the properly corresponding points will be conserved in the transition from the actual to the EF geometry. As already seen above [Eq. (A16)], in the general case where the stated conditions need not be satisfied, the relative curvature in the EF system, that is, the difference between the curvatures $1/R_1(P')$ of the trajectory at P' and $1/\infty$ of the earth's surface at $\overline{A}$, does not equal the relative curvature in the actual system, that is, the difference between $1/R(P)$ of the ray trajectory at P and $1/a$ of the earth's surface at A. It should be realized that the validity of the conservation depends on the fulfillment of the conditions $r \approx a$ and $\cos \theta \approx 1$.

Second, from Eq. (A16) it is seen that we will have $R_1(P') \gtrless 0$ for $\phi''(r) \gtrless 0$. Under the stated conditions this latter relation corresponds, from Eq. (12), to

$$-n' \gtrless \frac{1}{a} \approx 157 \text{ N unit/km} \quad .$$

Before closing the subsection we will make brief comments on the concept of the modified refractive index which plays a significant role in the treatment of various problems according to the EFM, and also on the connection between the elevation angles in the actual and the EF coordinate systems. The exact slope at P' of the trajectory in the EF system is given by

$$\frac{dh}{ds} = \frac{1}{a\phi'(r)} = \frac{r\sqrt{(rn)^2 - A^2}}{aA} = \left(1 + \frac{h}{a}\right) \frac{\sqrt{\tilde{n}_m(h)^2 - \tilde{A}^2}}{\tilde{A}} \quad , \tag{A18}$$

where

$$n_m(r) \equiv \frac{r}{a} n(r) = \left(1 + \frac{h}{a}\right) \tilde{n}(h) = \tilde{n}_m(h) \tag{A19}$$

defines the modified refractive index with $n(r) = \tilde{n}(h)$ and $\tilde{A} = A/a$. Therefore, in terms of the elevation angle $\underset{\sim}{\theta}(h)$ at P' we have

45

$$\tan \theta(h) = \left(1 + \frac{h}{a}\right) \frac{\sqrt{\tilde{n}_m(h)^2 - \tilde{A}^2}}{\tilde{A}} \quad .$$

If our attention is confined to the case where $h/a \ll 1$, the above relation becomes equivalent to

$$\tilde{n}_m(h) \cos \underset{\sim}{\theta}(h) = \tilde{A} = \text{const} \quad .$$

Recall from Eq. (A10) that this represents the ray trajectory equation for a medium with refractive index $\tilde{n}_m(h)$ as given by Eq. (A19). To determine the relation between the elevation angles $\theta(r)$ in the actual geometry and $\underset{\sim}{\theta}(h)$ in the EF system we note that the slope in the former is given by

$$\tan \theta(r) = \frac{dr}{r \, d\phi} = \frac{a}{r} \frac{dh}{ds} \quad ,$$

where use has been made of Eq. (A14). Since dh/ds is the slope of the trajectory in the EF system and hence is equal to $\tan \underset{\sim}{\theta}(h)$ we obtain the desired connection:

$$\tan \underset{\sim}{\theta}(h) = \frac{r}{a} \tan \theta(r) \Big|_{r=a+h} \quad .$$

Under the conditions of practical interest we may make the approximation that the factor r/a is unity by dropping the contribution from h/a, leading to the approximation $\underset{\sim}{\theta}(h) = \theta(a + h)$. This means, in particular, that the take-off and arrival angles determined experimentally may be identified with the corresponding angles that can be calculated in the EF system. We should note, on the other hand, that the factor r/a in Eq. (A19) must not be approximated by unity. This is because the propagation phenomena could depend sensitively on a relatively small change in the refractivity so that it also becomes necessary to retain the contribution from h/a even though this number may be very small in comparison to unity.

A2.3 Ray-Straightening Transformation

The transformation from the actual geometry to the RS system can be carried out in a manner analogous to the EF transformation. Namely, we imagine an observer who measures the distance travelled l and the depth to the earth's surface p by moving along the ray path in the actual geometry. When a rectangular coordinate system (l, p) [shown in solid curves in Figure A1(c)] is constructed it

46

describes the event in the RS coordinate system. Consider a point $Q'(\ell, p)$ on the transformed curve for the earth's surface and call the radius of curvature there $R_2(Q')$. The radius of curvature can be found in a way parallel to the EF case. First, from Figure A1(a) we note the geometrical relation

$$d\ell = dr / \sin \theta$$

from which we obtain

$$\ell'(r) = \frac{rn}{\sqrt{(rn)^2 - A^2}} \quad , \tag{A20}$$

$$\ell''(r) = - \frac{A^2 (rn)'}{\left[(rn)^2 - A^2\right]^{3/2}} \tag{A21}$$

and

$$\ell(r) = \int_{r_1}^{r} \frac{dr \, rn}{\sqrt{(rn)^2 - A^2}} \quad .$$

Next, we require the expression for $p(r)$. The simplest way to find this is to note that $\angle OPQ = \theta$ from which one can obtain directly that

$$p(r) = r \cos \theta - \sqrt{a^2 - r^2 \sin^2 \theta} \quad . \tag{A22}$$

To determine $R_2(Q')$ let us consider the mirror image [shown in the chained-lines in Figure A1(c)] of the RS picture outlined above. If the same letters ℓ and p are used for this new system, the radius of curvature $R_2''(Q'')$ at Q'' will be given, in accordance with our sign convention, by

$$R_2''(Q'') = - \frac{\left[1 + p'(\ell)^2\right]^{3/2}}{p''(\ell)} \quad .$$

47

Since we have

$$p'(\ell) = \frac{p'(r)}{\ell'(r)} \quad ,$$

$$p''(\ell) = \frac{d}{d\ell} p'(\ell) = \frac{p''(r)\ell'(r) - \ell''(r)p'(r)}{\ell'(r)^3} \quad ,$$

where the prime refers to the derivative with respect to the argument, and obviously $R_2(Q') = -R_2''(Q'')$, we obtain

$$R_2(Q') = + \frac{(\ell'^2 + p'^2)^{3/2}}{\ell'p'' - p'\ell''} = \frac{\left[1 + (1 - \xi^2)p'^2\right]^{3/2}}{(1 - \xi^2)p'' + \xi^2 p'(rn)'/rn} \quad . \tag{A23}$$

On the right-hand side of this equation, ℓ and p are considered as functions of r, and use has been made of Eqs. (A20)-(A22). As before, using Eq. (A13) we obtain the following relation from Eq. (A23)

$$\frac{1}{\infty} - \frac{1}{R_2(Q')} = \frac{1}{R(P)w_p(r)} - \frac{1}{aw_a(r)} \quad . \tag{A24}$$

where

$$w_p(r) = \frac{\left[1 + (1 - \xi^2)p'^2\right]^{3/2}}{\xi p'}$$

$$w_a(r) = \frac{\left[1 + (1 - \xi^2)p'^2\right]^{3/2}}{a\left[p'' - \xi^2(p'' - p'/r)\right]} \quad .$$

Under the conditions of practical interest mentioned earlier Eq. (A24) reduces to

$$\frac{1}{\infty} - \frac{1}{R_2(Q')} \approx \frac{1}{R(P)} - \frac{1}{a} \quad . \tag{A25}$$

since Eq. (A22) which now reads $p(r) \approx r - a = h$ gives rise to

$$p'(r) \approx 1 \quad \text{and} \quad p''(r) \approx 0 \tag{A26}$$

48

so that we have $w_p \approx 1$ and $w_a \approx 1$. In Eq. (A25) we see again the conservation of the relative curvature between the actual and the RS geometries. We might mention that this relation has sometimes been introduced into the literature without due statement about its condition of validity. We believe it worth noting that, like Eq. (17) and the relation

$$R_2(Q') \approx -R_1(P')$$

that follows from comparing Eqs. (A17) and (A25), it is of only limited validity. The relation

$$R_1(P') \approx -R_2(Q') \approx \frac{1}{1/R(P) - 1/a}$$

may be re-expressed in various familiar forms. Thus, by defining the lapse rate of the refractive index by $\mathcal{L} = -n'$ and noting that $n = 1$ and $\cos\theta = 1$ for all practical purposes we have

$$R_1(P') \approx \frac{1}{\mathcal{L} - 1/a} \approx -\frac{1}{n_m'} \quad ,$$

where use has been made of Eq. (A19). For the special case of $n' = $ const, the above expressions for $R_1(P')$ reduce to those given in Ref. 2. When Eq. (A13) is used we have

$$R_2(Q') \approx a \cdot \frac{1}{1 + an' \cos\theta/n} \equiv a \cdot k(r) \equiv a_e(r) \quad .$$

In the case of $n' = $ const, the approximately constant values of $a_e(r)$ and $k(r)$, written as a_e and k and called the equivalent earth radius and the earth radius factor, respectively, are of considerable utility in the discussion of wave propagation problems according to the RSM. In particular, when $\mathcal{L} \approx 1/4a \approx 40$ N unit/km which is customarily considered to correspond to the so-called standard atmosphere, we obtain the familiar value of $a_e = (4/3)a$. Before discussing the RS coordinate system employed in Ref. 3 we should point out the relation between the elevation angle $\theta(r)$ in the actual geometry (see Figure A1(a)) and the corresponding angle called $\varrho(p)$, measured positive in the direction from the earth's surface toward the ray trajectory, in the RS geometry (see Figure A1(c)). We have then

49

$$\tan \underline{\theta}(p) = \frac{dp}{d\mathit{l}} = \frac{p'(r)}{\mathit{l}'(r)} \quad .$$

With $\mathit{l}'(r)$ given by Eq. (A20) and $p'(r) \approx 1$ we obtain

$$\tan \underline{\theta}(p) \approx \frac{\sqrt{(rn)^2 - A^2}}{rn} = \sin \theta(r) \quad .$$

For small angles, this is equivalent to $\underline{\theta}(p) \approx \theta(r)$. That is, under the conditions of our interest we may identify the angle $\underline{\theta}(p)$ with the experimentally measurable angle $\theta(r)$. Recalling the similar relation $\underline{\theta}(h) \approx \theta(r)$ for the EF system we see that we may use the measured take-off or arrival angle as the corresponding angle in either the EF or RS system. In the remainder of this subsection we will summarize the RS transformation employed in Ref. 3 by slightly rephrasing it to make it easier for us to understand. Consider a transformation which maps a point P with polar coordinates $(r, \overline{\phi})$ in the real geometry [Figure A1(a)] into another point P_e with new polar coordinates $(r_e, \overline{\phi}_e)$. Under general circumstances such a transformation from (r, ϕ) to (r_e, ϕ_e) would be represented by the functional relations $r_e = F(r, \phi)$ and $\phi_e = G(r, \phi)$, where for convenience we introduced $\phi = \pi/2 - \overline{\phi}$ and $\phi_e = \pi/2 - \overline{\phi}_e$. Let us specialize the transformation to the case where

$$r_e = F(r)$$

$$\phi_e = \frac{a}{F(a)} \phi \quad .$$

Here $F(\cdot)$ is a function the form of which is yet to be determined. The first equation tells us that a circle in the original geometry is transformed into another circle in the new coordinate system. In the second equation, a stands for a conveniently defined earth radius, not necessarily equal to the customarily adopted value of about 6370 km, such as the radial distance up to the height of the layer interface. What the second equation means physically is simply that the arc length $s = a\phi$ and $s_e = F(a)\phi_e$ in the original and transformed systems, respectively, are equal. If we note the geometrical relations

$$\tan \theta(r) = \frac{dr}{rd\phi(r)} \tag{A27}$$

and

$$\tan \theta_e (r_e) = \frac{dr_e}{r_e \, d\phi_e (r_e)} \tag{A28}$$

and demand that the angle $\theta_e (r_e) = \theta_e (F(r)) \equiv \overline{\theta}(r)$ be identical to $\theta(r)$, then Eqs. (A27) and (A28) lead to a differential equation for the unknown function F given by

$$\frac{rF'(r)F(a)}{aF(r)} = 1 \quad . \tag{A29}$$

This has to be solved under an appropriate boundary condition. One way to do this is to regard Eq. (A29) as a differential equation for a function defined by $f(r) = rF(r)$. Its solution is of the form

$$f(r) = (cr)^{2-\gamma} \quad , \tag{A30}$$

where c is the integration constant and γ, given by

$$\gamma = 1 - \frac{a^2}{f(a)}$$

is another constant which characterizes the atmosphere, as will be seen below. The constant c can be given in terms of γ by using the expression for f(a) obtainable from Eq. (A30). In this way we can determine F as

$$r_e = F(r) = \frac{r}{1-\gamma} \left(\frac{a}{r}\right)^\gamma = \frac{a}{1-\gamma} \left(\frac{a}{r}\right)^{\gamma-1} \quad . \tag{A31}$$

For $r = a$ the above equation gives

$$a_e \equiv F(a) = \frac{a}{1-\gamma} \quad . \tag{A32}$$

So far there is nothing in the above transformation to indicate that the ray trajectory in the new system will be a straight line. To see that it can be under appropriate conditions let us recall the ray equation for the original geometry: $rn(r) \cos \theta(r) = $ const. First, note from Eq. (A31) that we have

51

$$\left(\frac{a}{r}\right)^{\gamma} = \left[\frac{(1-\gamma)r_e}{a}\right]^{\gamma/(\gamma-1)}$$

and

$$r = a\left[\frac{(1-\gamma)r_e}{a}\right]^{-1/(\gamma-1)} \quad .$$

If the refractive index is restricted to a class of functions of the form

$$n(r) = n(a)\left(\frac{a}{r}\right)^{\gamma} \quad , \tag{A33}$$

then the ray equation in the original system gives rise to the relation

$$r_e \cos \theta_e = \text{const}$$

in the transformed system, where use has been made of the relation $\theta(r) = \theta_e(r_e)$. Note that the relation just derived represents the equation for a straight line. Thus, we see that the transformation from (r, ϕ) to (r_e, ϕ_e) that has been employed will describe an RS transformation for a class of refractive index of the form of Eq. (A33). A question remains: What constant value of the refractive index will cause propagation along a straight line? To answer this question we recognize that a refractive index of the form of Eq. (A33) can make practical sense only when $r \approx a$. In that case we have $(a/r)^{\gamma} \approx 1$ regardless of the value of γ and hence $n(r) \approx n(a)$. That is, choosing almost any value of $n(r)$ for which $r \approx a$ will make no difference. In Ref. 3 the authors use the value at the height of the layer interface to calculate the time delay, which will be perfectly acceptable.

The significance of the constant γ that characterizes the atmosphere may be found in the following way. For an atmosphere with constant gradient of the refractive index we have for $r - a = h \ll a$,

$$n(r) = n(a) + n'(h) = n(a)(1 - \alpha h) \approx n(a)\left(\frac{a}{r}\right)^{a\alpha}$$

Comparing this with Eq. (A33) we find that

$$\gamma = a\alpha$$

52

Having examined the transformation employed in Ref. 3 we may observe that it represents a subset of the more general RS transformation discussed in Section A2.3. We say this because the transformation is valid only for the case where the transformed surface of the earth has a constant radius of curvature, whereas the radius $R_2(Q')$ in Section A2.3 need not be constant. Only when the ray trajectory remains almost horizontal and close enough to the earth's surface, and when the refractive index has a constant gradient, does our general RS system reduce to the one used in Ref. 3. Since we will be concerned exclusively with the circumstances in which the conditions just mentioned prevail, the RS transformation in Ref. 3 will be seen to be an appropriate one to be employed for the analysis.

Appendix B

B1. THE EFM

In this method the earth's surface is flat and the ray trajectory is curved. For an atmospheric layer with a constant refractive-index gradient, $n' = -\alpha =$ const, the ray trajectory is given, under the assumption that $r \approx a$ and $\cos \theta \approx 1$, by a circular arc whose radius is

$$R = \frac{1}{\alpha - 1/a} \quad . \tag{B1}$$

The elevation angle $\underset{\sim}{\theta}(h)$ at an arbitrary point on the ray trajectory in this system is related to the elevation angle $\theta(r)$ in the actual system (see A2.2) by

$$\tan \underset{\sim}{\theta}(h) = \frac{r}{a} \tan \theta(r) \Big|_{r=a+h} \quad .$$

Therefore, under the conditions of our interest we may set

$$\underset{\sim}{\theta}(h) \approx \theta(a + h) \quad . \tag{B2}$$

B2. THE RSM

Here the ray trajectory is represented by a collection of straight line segments that may be rectified into a single straight line, while the earth's surface, layer interface, etc., and other lines are transformed into curved lines. According to the particular version of the RS system employed by the Signatron workers the earth's surface (radius a) and the layer interface (radius $r_D = a + h_D$) in the plane of the ray trajectory are transformed, respectively, [see Eq. (A31)] into circles of radii

$$a_e \equiv F(a) = \frac{a}{1 - \gamma} \quad \text{and} \quad r_{eD} \equiv F(r_D) = \frac{a}{1 - \gamma} \left(\frac{a}{r_D}\right)^{\gamma - 1} . \tag{B3}$$

The elevation angle $\theta_e(r_e)$, at an arbitrary point on the ray trajectory in the RS system, is exactly equal to the elevation angle $\theta(r)$ at the corresponding point in the actual system [see below Eq. (A28)]:

$$\theta_e(r_e) = \theta(r) . \tag{B4}$$

B3. COMPARISON OF RESULTS

We can now proceed to examine an event occurring in the actual system (Figure B1(a)) as seen in the EF and RS systems (Figures B1(b) and B1(c)).

For the EF system we have from Figure B1(b) and Eq. (B2)

$$L_1 = R_f(\sin \theta_D - \sin \theta_T)$$

$$S_1' \approx R_f(\theta_D - \theta_T) . \tag{B5}$$

On the other hand, from Figure B1(c) we have

$$L_1' = F(r_D)(\theta_D - \theta_T)$$

$$X_1 = F(r_D) \sin \theta_D - F(r_T) \sin \theta_T ,$$

where $r_T = a + h_T$. By using the relation $F(r) = F(r_D) - d_T$ we may write $X_1 = F(r_D)(\sin \theta_D - \sin \theta_T) + d_T \sin \theta_T$ where the first term on the right hand side equals X_1'. For $h_D/a \ll 1$ we have $F(r_D) = F(a)(a/r_D)^{\gamma - 1} \approx F(a) = a_e$ so that we may write

56
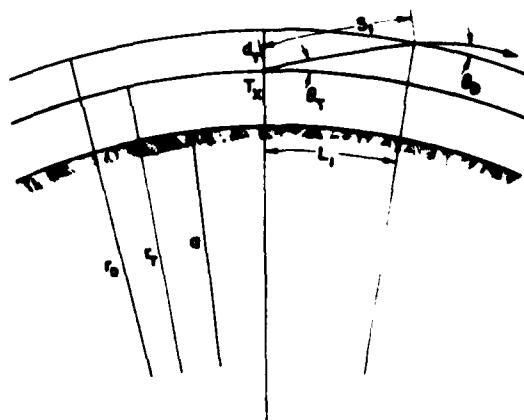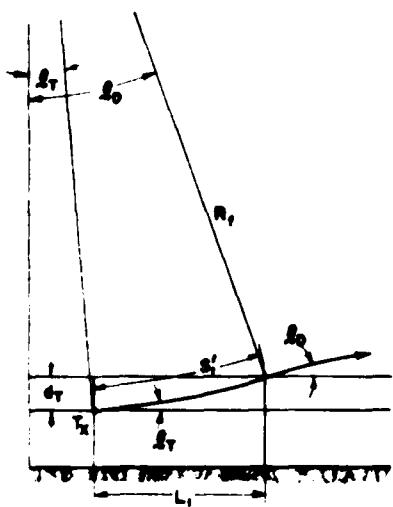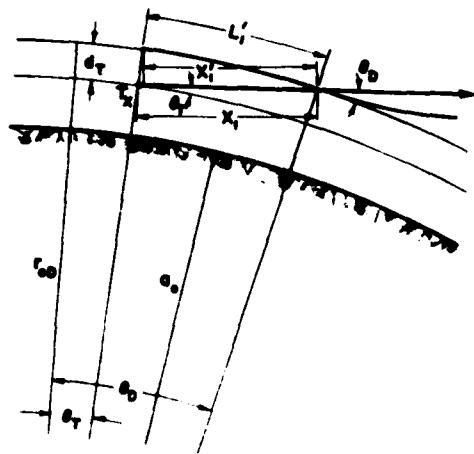
Figure B1. Path Description in (a) the Actual; (b) Earth-Flattening; and (c) Ray-Straightening Systems

57

$$L_1' = a_e(\theta_D - \theta_T)$$

$$\lambda_1 = a_e(\sin \theta_D - \sin \theta_T) \quad . \tag{B6}$$

The quantity R_f in Eq. (B5) is the radius of curvature of the ray in the standard atmosphere with $\alpha = 1/4a$ so that we have $R_f = | 1/(1/4a - 1/a)| = 4a/3$. The radius a_e of Eq. (B6) is given by the first of Eqs. (B3) where γ takes on the value of $1/4$ for the standard atmosphere. Therefore, we have
$a_e = a/(1 - 1/4) = 4a/3 = R_f$.

A comparison of Eqs. (B5) and (B6) shows clearly that the roles of the ray path and the layer interface are interchanged between the EFM and the RSM, that is, the relevant figures in the two methods are the mirror images of each other. Extending the analogous argument to all the other segments of the ray trajectory, we may conclude that the statement just derived remains valid, in general.

MISSION
of
Rome Air Development Center

RADC plans and executes research, development, test and selected acquisition programs in support of Command, Control Communications and Intelligence (C^3I) activities. Technical and engineering support within areas of technical competence is provided to ESD Program Offices (POs) and other ESD elements. The principal technical mission areas are communications, electromagnetic guidance and control, surveillance of ground and aerospace objects, intelligence data collection and handling, information system technology, ionospheric propagation, solid state sciences, microwave physics and electronic reliability, maintainability and compatibility.

END

FILMED

8-83

DTIC